1-1-2017

# Activity Dependent Changes In Functional And Morphological Characteristics Among Presympathetic Neurons Of The Rostral Ventrolateral Medulla

Daniel J. Huereca
*Wayne State University,*

# ACTIVITY DEPENDENT CHANGES IN FUNCTIONAL AND MORPHOLOGICAL CHARACTERISTICS AMONG PRESYMPATHETIC NEURONS OF THE ROSTRAL VENTROLATERAL MEDULLA

by

**DANIEL JOSEPH HUERECA**

**DISSERTATION**

Submitted to the Graduate School

of Wayne State University,

Detroit, Michigan

in partial fulfillment of the requirements

for the degree of

**DOCTOR OF PHILOSOPHY**

2017

MAJOR: PHARMACOLOGY

Approved By:

_____

Advisor Date

_____

_____

_____

_____

_____

## DEDICATION

I dedicate this work to my wife Robyn, who put up with me through all of this, my family, who put up with rarely hearing from me through all of this, and my brother, who supported me for as long as he could. Thanks, everybody.

## ACKNOWLEDGEMENTS

There are many people who helped make this work possible, and it likely would not have been possible without the support of following people, in no particular order: Dr. Patrick Mueller, who gave me a place to work and trained me to be a better scientist, the current and former members of my dissertation committee, Drs. Genene Holt, Noreen Rossi, Raymond Mattingly, Nicholas Davis, Roy McCauley, and Sokol Todi; Toni Azar, who taught me almost everything I know about animal surgeries; Konstandinos Bakoulas, who shared in some of these experiments; Drs. Ida Llewellyn-Smith, Bruce Berkowitz, Farhad Ghoddoussi, and Stephen DiCarlo, who shared equipment, and most importantly, knowledge; Qijing Yu from the Wayne State University Research Design and Analysis Unit; the staff of the Physiology and Pharmacology departments, especially Christine Cupps; the current and former members of the Mueller laboratory who contributed to this project, Dr. Bozena Fyk-Kolodziej, Dr. Maryetta Dombrowski, Dr. Madhan Subramanian, Dr. Nicholas Mischel, Zachery Krease, Marcel Mic, Benjamin Maynard, and the many other undergraduate and high-school students who have helped with this project and laboratory upkeep; and, of course, my family.

## TABLE OF CONTENTS

## LIST OF FIGURES

## LIST OF ABBREVIATIONS

| | |
|---|---|
| Cardiovascular disease | CVD |
| Caudal pressor area | CPA |
| Caudal ventrolateral medulla | CVLM |
| Cerebrospinal fluid | CSF |
| Facial nucleus, caudal pole | FN0 |
| Gamma-aminobutyric acid | GABA |
| Intraperitoneal | i.p. |
| Intravenous | i.v. |
| Intermediolateral nucleus of the spinal cord | IML |
| Lateral tegmental field | LTF |
| Mean arterial pressure | MAP |
| Manganese enhanced magnetic resonance imaging | MEMRI |
| Magnetization prepared rapid acquisition gradient echo | MPRAGE |
| Magnetic resonance imaging | MRI |
| Noradrenergic cell group A5 | A5 |
| Nucleus ambiguus | NA |
| Nucleus tractus solitarius | NTS |
| Proton density weighted gradient echo | PDGE |
| Paraventricular nucleus of the hypothalamus | PVH |
| Phenylephrine | PE |
| Phenylethanolamine N-methyltransferase | PNMT |
| Pyramidal tract | Pyr |

| | |
|---|---|
| Region of interest | ROI |
| Rostral ventrolateral medulla | RVLM |
| Rostral ventromedial medulla | RVMM |
| Sympathetic nerve activity | SNA |
| Spinal trigeminal tract | SP5 |
| Sodium nitroprusside | SNP |
| Sympathetic preganglionic neuron | SPN |
| Splanchnic sympathetic  nerve activity | SSNA |
| Repetition time | TR |

# CHAPTER 1 - INTRODUCTION

Cardiovascular disease (CVD), made up of a number of interrelated disorders, is the world-wide leading cause of death among adults (Mendis, et al., 2011). According to the World Health Organization, CVD makes up nearly one third of all deaths from any cause, and nearly one half of all deaths not caused by communicable diseases (Mendis, et al., 2014). In the United States, projections from the American Heart Association estimate that 17% of all healthcare costs are spent treating CVD, and the total annual cost of CVD in the United States is expected to be approximately $700 billion by 2020, and nearly $1.1 trillion by 2030 (Heidenreich, et al., 2013). Interestingly, a sedentary lifestyle, or lack of sufficient physical activity, has been implicated as a major, preventable, risk factor for developing a number of disorders which fall under the category of CVD (Thom, et al., 2006). Conversely, increased levels of physical activity have been associated with a reduced probability of developing CVD, and have been associated with a reduction in mortality in people who suffer from CVD (Myers, et al., 2002;Luo, et al., 2017).

One key factor linking a sedentary lifestyle to an increased likelihood of developing CVD (Figure 1) is an increased level of sympathetic nerve activity (SNA) (Malpas, 2010;Mueller, 2010). The sympathetic nervous system, commonly referred to as being responsible for the “fight or flight” reaction, is tonically active and is constantly modifying levels of SNA from heart beat to heart beat, to maintain homeostasis, or to change levels of sympathetic tone to meet physiological demands (Dampney, et al., 1987;Dean, et al., 1992;Lovick and Hilton, 1985;Lovick, 1987). Multiple animal models have demonstrated associations between risk factors for CVD and increases in SNA. For instance, rats fed high fat or high salt diets are known to have increased SNA

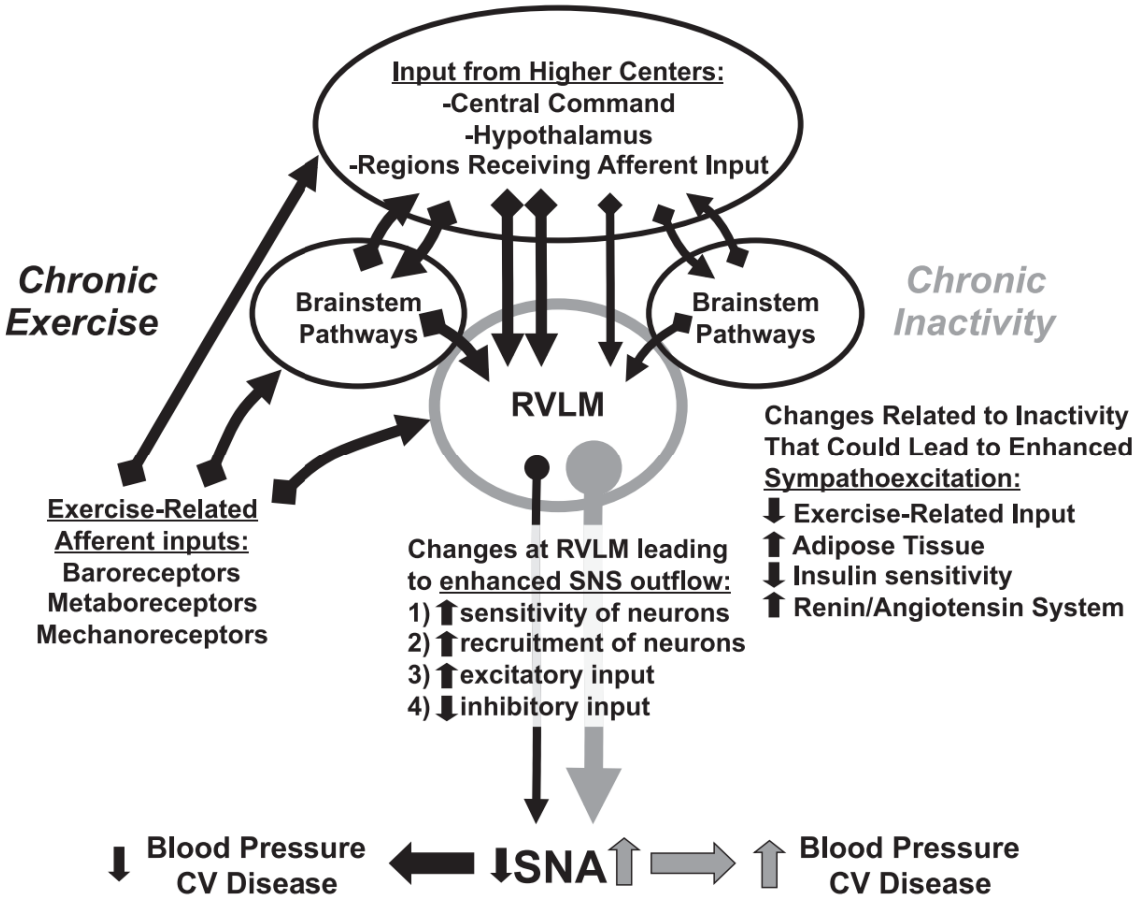


**Figure 1. Diagram illustrating the role of the RVLM in the relationships between SNA and sedentary versus physically active conditions.** Sedentary conditions can result in neuroplastic changes in the RVLM, leading to increases in SNA. (From Mueller 2010)

compared to rats fed normal diets (Iwashita, et al., 2002;Muntzel, et al., 2012;Morgan, et al., 1995). Furthermore, Obese Zucker rats have been shown to exhibit increased splanchnic SNA (SSNA) and a blunted ability to reduce it, compared to their lean counterparts, when challenged with increases in arterial pressure (Huber and Schreihofer, 2010;Huber and Schreihofer, 2011). Similarly, rats exposed to chronic intermittent hypoxia, a model frequently used to simulate obstructive sleep apnea in humans, have been shown to have enhanced increases in SSNA following stimuli such as electrical stimulation of the sciatic nerve, acute hypoxia, and activation of the chemoreflex compared to control rats (Silva and Schreihofer, 2011). These are just a

few examples from a much larger body of literature which demonstrate a clear link between risk factors for CVD and increases in SNA.

The major regulator of SNA is a region of the brainstem known as the rostral ventrolateral medulla (RVLM) (Ross, et al., 1984b; Guyenet, 2006; Schreihofer and Guyenet, 2002). The RVLM, in rats, has been traditionally defined as an approximately 1 mm long region of the brainstem, extending caudally from the caudal pole of the facial motor nucleus, and found ventral to the nucleus ambiguus, lateral to the pyramids, and medial to the spinal trigeminal tract, though more recent studies have demonstrated that the RVLM extends several hundred micrometers rostral to the caudal pole of the facial nucleus (Llewellyn-Smith and Mueller, 2013; Ruggiero, et al., 1989; Schreihofer and Guyenet, 2000b). The rostral portion of the RVLM, extending approximately 500μm caudal from the caudal pole of the facial nucleus, has been of special interest to groups studying control of SNA (Figure 2). This region of the medulla has been shown to

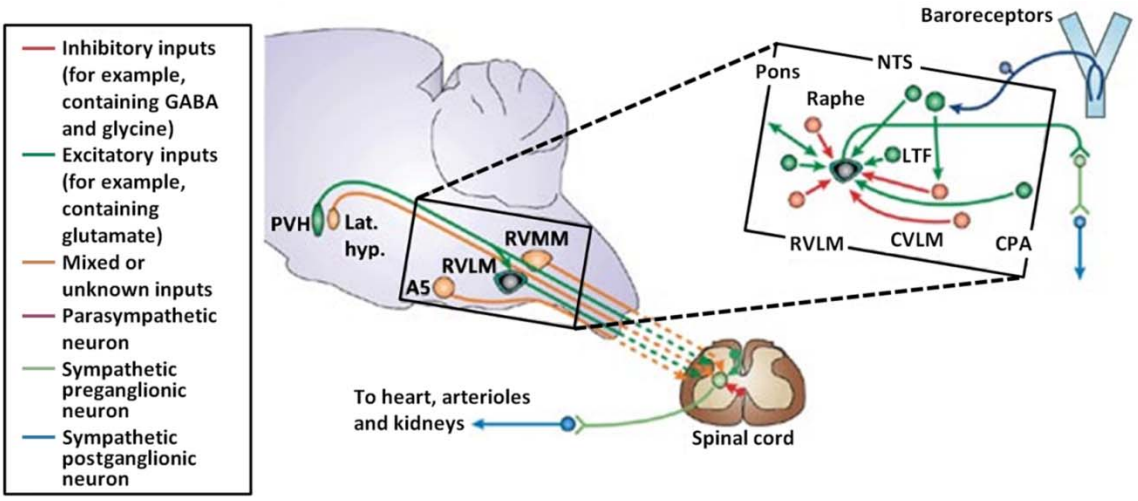


**Figure 2. Diagram illustrating the role of the RVLM in integrating physiological signals to generate sympathetic tone.** The RVLM receives and integrates excitatory and inhibitory inputs and stimulate SPNs via glutamatergic monosynaptic connections. A5, noradrenergic cell group A5; CPA, caudal pressor area; Lat. hyp., lateral hypothalamus; LTF, lateral tegmental field; NTS, nucleus tractus solitarius; PVH, paraventricular nucleus of the hypothalamus; RVMM, rostral ventromedial medulla; GABA, gamma-aminobutyric acid. (Modified from Guyenet 2006)

contain two main types of bulbospinal, spinally-projecting, neurons, Phenylethanolamine N-methyltransferase (PNMT)-positive C1 neurons and PNMT-negative non-C1 neurons. These neurons are frequently referred to as “presympathetic” because they regulate SNA via axons that project into the intermediolateral column of the spinal cord (IML) and directly activate sympathetic preganglionic neurons via monosynaptic connections (Oshima, et al., 2006; Schreihofer and Guyenet, 2002; McAllen, et al., 1994). The neurons of the RVLM receive both excitatory and inhibitory inputs from regions of the brain involved in control of the autonomic nervous system, such as the paraventricular nucleus of the hypothalamus (PVH), nucleus tractus solitarius (NTS), and the caudal ventrolateral medulla (CVLM) (Guyenet, 2006). There is also evidence that the activity of neurons within the RVLM can be modulated by direct and indirect input from higher centers in the forebrain, such as the amygdala and the medial prefrontal cortex (Owens, et al., 1999; Cassell and Gray, 1989). Finally, the RVLM is known to respond to changes in concentrations of solutes and neurohormonal factors present in cerebrospinal fluid, such as glucose, leptin, vasopressin, and angiotensin II (Dampney, et al., 2002; Verberne and Sartor, 2010; Ito, et al., 2003; Barnes and McDougal, 2014; Kc, et al., 2010). Clearly, the RVLM serves to integrate signals from a wide variety of sources in order to regulate sympathetic tone.

One of the major roles of the RVLM is that of modifying blood pressure via control of SSNA. RVLM neurons are tonically active and maintain splanchnic sympathetic tone in part by activation of sympathetic preganglionic neurons (SPNs) via release of glutamate in the IML at the T9-T10 level of the spinal cord (Oshima, et al., 2006; Schreihofer and Guyenet, 2002). The terminals of these SPNs release acetylcholine onto the dendrites of postganglionic vasomotor neurons. In turn,

splanchnic sympathetic postganglionic vasomotor neurons release norepinephrine to maintain contraction of the smooth muscle surrounding splanchnic blood vessels. This increase in venous smooth muscle tone serves to divert blood out of the splanchnic reservoir and into the systemic circulation. In dogs, the splanchnic reservoir has been shown to contain up to half of total blood volume, enabling a large amount of blood to be redistributed into arteries when necessary (Delorme, et al., 1951). The result of this redistribution of splanchnic venous blood, caused by activation of RVLM neurons, is an increase in arterial pressure.

When arterial pressure is high, neurons in the baroreceptors located in the aortic arch and the carotid sinus sense the stretching of the arterial wall, and release glutamate from their terminals in the NTS (Schreihofer and Guyenet, 2002). This release of glutamate within the NTS activates glutamatergic, or glutamate-releasing, neurons that project from the NTS to the CVLM (Zhang and Mifflin, 1997). These NTS neurons then increase activity of neurons in the CVLM which produce the inhibitory neurotransmitter γ–amino butyric acid (GABA) (Schreihofer and Guyenet, 2003). These GABA-releasing (GABAergic) CVLM neurons project to, and release GABA into the RVLM (Agarwal and Calaresu, 1991; Li, et al., 1991). The effect of this GABA is to decrease the excitability of RVLM neurons, causing a decrease in the frequency of, or a cessation of, action potentials, ultimately resulting in a decrease in sympathetic tone and arterial pressure (Li, et al., 1991). Because RVLM neurons are tonically active despite being under GABA-dependent inhibition, SNA and arterial pressure can be increased or decreased as needed via increases or decreases in RVLM neuronal activity, as a result of decreases or increases in GABA release within the RVLM, respectively (Dampney, et al., 1988; Cravo and Morrison, 1993).

Recent research has shown that, much like sympathetic nerve activity itself, the RVLM demonstrates functional and morphological changes as a result of exposure to different conditions (Mischel and Mueller, 2011;Mischel, et al., 2014; Subramanian and Mueller, 2016). For example, our laboratory has previously demonstrated that in a rat model, rats exposed to sedentary conditions exhibit a greater level of SSNA than is seen in physically active rats when challenged with decreases in arterial pressure (Mischel and Mueller, 2011). This effect was observed following intravenous infusion of the nitric oxide donor, sodium nitroprusside, presumably due to differences in RVLM sensitivity to excitatory stimuli. More directly supporting the idea that levels of physical activity alter the function of the RVLM, our laboratory has also shown that microinjection of the excitatory amino acid glutamate directly into the RVLM causes a greater increase in SSNA in sedentary versus physically active rats (Mischel and Mueller, 2011). Our laboratory has also reported that in presympathetic RVLM neurons, expression of the gene coding for the GluR3 subunit of the excitatory AMPA-type glutamate receptor is inversely correlated with running distance (Subramanian, et al., 2014). The correlation between decreased physical activity and increases in GluR3 mRNA expression suggests a potential mechanism for increased excitability of RVLM neurons, and for the enhanced SSNA observed in sedentary versus physically active rats following microinjection of glutamate into the RVLM. This indicates that increased physical activity may contribute to decreased sensitivity to excitatory stimuli via regulation of glutamate receptors. Finally, while other studies have demonstrated that the dendritic structure of neurons is associated with levels of physical activity in some areas of the brain involved in cardiorespiratory function (Nelson, et al., 2005; Nelson, et al., 2010), our group has demonstrated that similar changes also occur within the RVLM. More

specifically, our group has reported that rats that have been exposed to sedentary conditions exhibit greater dendritic arborization and greater dendritic length among the C1 subtype of presympathetic neurons than are seen in physically active rats (Mischel, et al., 2014). Taken together, these data suggest that differences in levels of physical activity can lead to morphological and functional differences in presympathetic neurons within the RVLM (Mischel, et al., 2015). These condition-dependent differences in RVLM sensitivity may then result in different levels of SSNA following a sympathoexcitatory challenge. As increases in SNA result in increases in arterial pressure, these studies suggest a potential link between sedentary conditions and chronically elevated blood pressure, a risk factor for CVD in humans (Grassi, et al., 1994; Laterza, et al., 2007; Fisher, et al., 2009).

While it has been shown that sedentary versus physically active conditions can result in different levels of SSNA following unloading of the baroreceptor or microinjection of excitatory amino acids directly into the RVLM (Mischel and Mueller, 2011; Mischel, et al., 2014), evidence of the mechanism responsible for these differences between groups has been elusive. In essence, the questions to be answered are whether the reported changes in SSNA are associated with functional and structural neuroplasticity among RVLM neurons, and do these potential neuroplastic changes result in different baroreflex characteristics, e.g., increased activity at rest or during sympathoexcitation, or decreased inhibition during periods of elevated arterial pressure, following chronic exposure to chronic sedentary versus physically active conditions?

While there are no studies directly comparing the effects of chronic sedentary versus physically active conditions on the activity or baroreflex characteristics of

individual presympathetic RVLM neurons, some studies have looked at the effects of variables related to the acute response to exercise and CVD. For instance, Kajekar *et al.* demonstrated that post-exercise hypotension is associated with an acute decrease in activity among RVLM neurons lasting at least10 hours (Kajekar, et al., 2002). It is unclear how the inhibitory effects of acute physical activity on RVLM neurons could relate to models examining the effects of long-term physical activity. However, the most logical hypothesis would be that chronic exposure to acute bouts of physical activity would result in neuroplastic changes that cause chronic inhibition of RVLM neurons, making them less active than comparable neurons in chronically sedentary rats.

In contrast to the acute effects of physical activity and chronic effects of diet, other groups studying models relating to CVD that are known to cause changes in SNA baroreflex responses have reported finding no effect on baseline or maximum activity of presympathetic RVLM neurons. For instance, Pedrino et al. reported no significant differences between resting or maximal firing rates of presympathetic RVLM neurons in angiotensin-II salt hypertensive rats versus normotensive controls (Pedrino, et al., 2013). Similarly, How and colleagues did not observe differences in maximal firing rates of presympathetic RVLM neurons between obesity prone and obesity resistant rats following 13-15 weeks of being fed a high-fat diet (How, et al., 2014). However, they did report that the neurons were significantly less inhibited by increases in arterial pressure in obesity prone versus obesity resistant animals, suggesting the potential for inappropriately high level of sympathetic tone, a risk factor for CVD (Paton, et al., 2005).

Taken together, these studies suggest that lifestyle and dietary conditions may have the potential to result in both acute and long-term neuroplastic changes in the function of RVLM neurons, such as increases in sensitivity to excitation or decreases in

sensitivity to inhibition. The question then is whether the previously mentioned effects of sedentary conditions on SSNA (i.e., increased resting activity and enhanced responses to sympathoexcitatory stimuli) are consistent with corresponding changes in neurons located within the RVLM. The studies presented in this dissertation investigated the extent to which sedentary versus physically active conditions affect the tonic activity and baroreflex regulation of individual neurons within the RVLM, and the general level of neuronal activity within the RVLM as a whole. The overall hypothesis of this research is that sedentary conditions enhance the activity of presympathetic RVLM neurons and increase their sensitivity to changes in arterial pressure.

**Specific Aim 1:** Examine functional and structural mechanisms by which bulbospinal RVLM neurons contribute to enhanced sympathoexcitation in sedentary versus physically active rats

Hypothesis 1.1: Single unit recordings of presympathetic RVLM neurons *in vivo* will reveal a higher basal activity and greater responsivity to sympathoexcitatory stimuli in sedentary rats.

Hypothesis 1.2: Dendritic arborization will positively correlate with activity and excitability of presympathetic RVLM neurons that have been juxtacellularly labeled *in vivo.*

**Specific Aim 2:** Evaluate neuronal activity within the RVLM of sedentary and physically active rats using manganese enhanced magnetic resonance imaging (MEMRI)

Hypothesis: MEMRI will reveal greater neuronal activity in the RVLM of sedentary versus physically active rats and that this effect will develop over the course of 12 weeks.

# CHAPTER 2 - EXAMINATION OF FUNCTIONAL AND STRUCTURAL MECHANISMS BY WHICH BULBOSPINAL RVLM NEURONS CONTRIBUTE TO ENHANCED SYMPATHOEXCITATION IN SEDENTARY VERSUS PHYSICALLY ACTIVE RATS

## Introduction

Cardiovascular disease (CVD) is the leading cause of preventable death among adults in the United States of America (Thom, et al., 2006; Heidenreich, et al., 2013), and the leading cause of all death around the world (Mendis, et al., 2014). A growing body of research has shown that a sedentary lifestyle contributes to the development and progression of CVD (Krieger, et al., 2001; Zucker, et al., 2004; Booth, et al., 2007). While studies have examined how physical inactivity contributes to individual risk factors of CVD, a common mechanism behind these risk factors remains elusive. Recent publications have highlighted the link between physical inactivity and increases in sympathetic nerve activity (SNA), suggesting autonomic dysregulation as a potential underlying cause of CVD (Krieger, et al., 2001; Mischel, et al., 2014; Zucker, et al., 2004).

SNA is primarily regulated by a region of the brainstem known as the rostral ventrolateral medulla (RVLM) (Ross, et al., 1984b). The RVLM contains neurons which regulate SNA via axons that project to the intermediolateral cell column (IML) of the spinal cord to release glutamate onto sympathetic preganglionic neurons (SPNs) (Ross, et al., 1984a). Because the spinally-projecting neurons within the RVLM regulate SPNs, they are frequently referred to as presympathetic neurons (Schreihofer and Guyenet, 2000a; Schreihofer and Sved, 2011). A population of RVLM presympathetic neurons is tonically active and integrate excitatory and inhibitory signals from central and peripheral sources in order to maintain sympathetic tone. A change in the balance of excitatory versus inhibitory input to presympathetic neurons results in a change in their

release of glutamate onto SPNs, thus altering sympathetic tone, as dictated by changes in physiological demand (Dampney, et al., 1987; Dean, et al., 1992; Lovick and Hilton, 1985; Lovick, 1987). Previous work from our laboratory has shown an association between sedentary conditions and exaggerated increases in splanchnic SNA (SSNA) in rats (Mischel and Mueller, 2011). One potential mechanism for the observed differences in SNA between sedentary and physically active rats is a change in sensitivity to sympathoexcitatory stimuli within the rostral ventrolateral medulla (RVLM) (Mischel, et al., 2015). Supporting this observation, our group has shown that after 10-13 weeks of sedentary versus physically active conditions, an enhanced increase in SSNA is observed in sedentary rats following direct activation of the RVLM via microinjection of the excitatory amino acid glutamate (Mischel and Mueller, 2011).

While presympathetic RVLM neurons are known to be modulated by a variety of stimuli, the major factor controlling their activity is arterial pressure (Haselton and Guyenet, 1989; Lipski, et al., 1995; Schreihofer and Guyenet, 2002). Increases in arterial pressure activate baroreceptors located in the aortic arch and at the bifurcations of the carotid arteries, resulting in inhibition of presympathetic RVLM neurons (Lipski, et al., 1996; Guyenet, 2006). This inhibitory effect has been clearly demonstrated by eliciting decreases in SNA via direct electrical stimulation of baroreceptors afferents (Gonzalez, et al., 1983; Hayward, et al., 2002). Conversely, unloading of the baroreceptor, via decreases in arterial pressure, results in disinhibition of presympathetic RVLM neurons and increases their action potential frequency, resulting in an increase in sympathetic tone (Mueller, et al., 2011; Schreihofer and Guyenet, 2000b; Kajekar, et al., 2002). Our laboratory has previously demonstrated that there are enhanced SSNA responses in sedentary compared to physically active rats

following either baroreceptor unloading (i.e. decreases in arterial pressure) or microinjection of the excitatory amino acid, glutamate, directly into the RVLM (Mischel and Mueller, 2011). This suggests that presympathetic RVLM neurons in sedentary rats have functional characteristics which make them more sensitive to sympathoexcitatory stimuli compared to those found in physically active rats. This proposed increase in sensitivity may lead to hyperactivity in the RVLM and increases in SNA, resulting in chronic increases in sympathetic tone, arterial pressure, and acute responses to sympathoexcitatory stimuli.

Consistent with the idea that differences in physical activity may result in functional neuroplastic changes among presympathetic RVLM neurons, our group has reported a negative correlation between running distance of physically active rats and expression of the gene coding for the glutamate receptor subunit GLUR3; these data suggest sedentary conditions may result in increased excitability of RVLM neurons (Subramanian, et al., 2014). Furthermore, our group has also reported that the C1 subtype of presympathetic RVLM neurons exhibit significantly greater dendritic arborization and length in sedentary versus physically active rats, suggesting the potential for greater synaptic input from afferent sources (Mischel, et al., 2014). Clearly, the RVLM offers an exciting opportunity to investigate functional and structural neuroplasticity which may underlie the differences in SNA that occur as a result of sedentary versus physically active animals, and may contribute to the development of cardiovascular disease in humans.

In this study we investigate differences in the morphology and baroreflex characteristics of presympathetic RVLM neurons, and examine their correlation to baroreflex characteristics of SSNA in sedentary and physically active rats. We have

used splanchnic nerve recording and single-unit extracellular recording of RVLM neurons to quantify their responses following pharmacologically-induced changes in blood pressure, as well as juxtacellular labeling to reconstruct the recorded neurons. We hypothesized that RVLM neurons would exhibit increased basal activity and baroreflex sensitivity in sedentary versus physically active rats (12-15 weeks spontaneous wheel running) and that physical activity would correlate with a reduction in dendritic arborization. To our knowledge, this is the first study to combine *in vivo* nerve and single-unit recordings from barosensitive RVLM neurons with juxtacellular labeling to examine relationships between SSNA, and the function and structure of presympathetic RVLM neurons in sedentary and physically rats.

## Methods

### *Ethical statement*

All protocols were approved by IACUC of Wayne State University and performed according to the guidelines published by the NIH and in the American Physiological Society's *Guiding Principles in the Care and Use of Animals.*

### *Animal model*

21 male Sprague Dawley rats (Harlan, Indianapolis, IN) weighing 75-100g upon arrival were randomly designated as sedentary or physically active and singly housed in polycarbonate cages under controlled temperature and light (12:12 light:dark cycle) conditions. Rats designated as physically active were allowed free access to in-cage running wheels while sedentary rats did not have access to running wheels. A bike computer (SigmaSport, Olney, IL) was used to monitor daily running wheel activity. At all times, rats had *ad libitum* access to tap water and food (Purina LabDiet 5001 Purina Mills, Richmond, IN). To eliminate potential acute effects of physical activity, running

wheels were removed from cages the day before experiments (Kajekar, et al., 2002;Kulics, et al., 1999).

***Surgical preparation***

After 10-15 weeks of physically active or sedentary conditions, animals were anesthetized with isoflurane (5% induction, 2% maintenance in 100% $O_{2;}$ Ohio Vaporizer, ASE, Gurnee, IL, USA) during surgical procedures. Animals were then instrumented with femoral arterial and venous catheters to record arterial pressure and administer drugs, respectively. A tracheostomy was performed and the trachea was cannulated to administer artificial ventilation (Inspira ASV, Harvard Apparatus, Holliston, MA). A small incision was made in the skin of the left cheek to expose the mandibular branch of the facial nerve. The left splanchnic nerve was exposed via a retroperitoneal incision, placed on silver wire electrodes, and secured by siloxane gel (S4, Bisico, Bielfeld, Germany). Rats were placed on a KOPF stereotaxic apparatus (Kopf Instruments, Tujunga, CA, USA) in the flat skull position (incisor bar lowered to 3mm below horizontal). A laminectomy was performed at the T2 vertebra to allow electrical stimulation in the intermediolateral cell column. A hole was drilled in the interparietal bone and the dura was retracted to allow insertion of extracellular recording electrodes. After surgical procedures were completed, isoflurane was gradually reduced during infusion of Inactin (R99 Syringe Pump, Razel, Saint Albans, VT; thiobutabarbital sodium, 100 mg/kg, i.v.). Supplemental anesthesia was administered as needed throughout the experiment in order to maintain suppression of the toe-pinch induced withdrawal reflex and gross increases in arterial pressure. Partial Pressure of blood $CO_2$ was monitored (Radiometer ABL5, Diamond Diagnostics, Holliston, MA, USA) and maintained by adjusting the rate of the ventilator. Animal internal body temperature was

monitored via rectal thermometer and maintained at 37°C via a polycarbonate warming pad connected to a warm water recirculator (HP-5057, Hallowell EMC, Pittsfield, MA; T/P500, Gaymar). After completion of experiments, animals were either euthanized via either overdose of FatalPlus (Vortech, Dearborn, MI) or transcardial perfusion.

***Extracellular recording of RVLM neurons***

Glass electrodes were pulled from capillary tubes (1B200-F4, WPI, Sarasota, FL, USA) using a Narishige PE-21, and filled with 2 M NaCl (2 MΩ resistance for facial field mapping, 4-8 MΩ for extracellular unit recording). Electrodes were then positioned in the brainstem using a hydraulic probe Microdrive (FHC, Bowdoin, ME).

A bipolar stimulating electrode was used to stimulate the mandibular branch of the facial nerve. The facial motor nucleus was located, and its shape was mapped, by detecting the field potentials caused by antidromic activation of the facial nerve (0.1-0.2 ms; 0.1-1.0 mA; S88FS Grass Technologies (West Warwick, RI); Stimulus Isolator (WPI A385 or Iso-Flex, A.M.P.I). The RVLM was identified by its position immediately caudal to the caudal pole of the facial nucleus and no attempts were made to record from neurons rostral to the caudal pole of the facial nucleus. For single-unit extracellular recordings, an intracellular amplifier (Neuroprobe 1600, A-M Systems, Sequim, WA) was used in bridge mode. A bipolar stimulating electrode was positioned in the intermediolateral cell column (IML) at T2 for antidromic activation of spinally projecting neurons. After pancuronium-induced paralysis (0.5-1.0 mg/kg with supplements to maintain paralysis), placement of the electrode in the IML was confirmed by increases in arterial pressure following electrical stimulation (>20 mmHg, 1s train, 0.2 ms pulse duration, 50 Hz, 0.5 mA). A subset of neurons was verified as spinally projecting by inducing antidromic action potentials by electrical stimulation (0.5 mA, 0.2 ms).

***Baroreflex testing***

The barosensitivity of neurons (n = 11) and splanchnic nerves from 10 physically active animals and neurons (n = 11) and splanchnic nerves from 11 sedentary animals was assessed by the change in the number of action potentials during i.v. infusion of 1 mg/mL phenylephrine to induce increases, and 1 mg/mL sodium nitroprusside to induce decreases in arterial pressure. Drugs were slowly given via i.v. catheter either by manual administration (n = 6 physically active rats, 3 sedentary rats) or by syringe pump (n = 4 physically active rats, 8 sedentary rats) in an effort to produce changes in MAP of 1-2 mmHg/s (Foley, et al., 2005; Moffitt, et al., 1998).

***Juxtacellular labeling***

A subset of neurons (n = 7 in 7 physically active animals, n = 4 in 4 sedentary animals) was labeled similar to the method described in Pinault 1996 (Schreihofer and Guyenet, 1997; Pinault, 1996; Toney and Daws, 2006). Neurons were recorded and assessed for barosensitivity using electrodes filled with 0.5 M sodium acetate and 5% Neurobiotin (Vector Laboratories, Burlingame, CA) in water (17-30 MΩ resistance). Following assessment of barosensitivity, neurons were juxtacellularly labeled using 200 ms anodal current pulses at 2.5 Hz (50% duty cycle). Current intensity was gradually increased until action potentials were entrained to current pulses.

***Histological processing of neurons labeled juxtacellularly in vivo***

After juxtacellular labeling, depth of anesthesia was reconfirmed by toe pinch. The chest was opened and heparin (1000 IU) was injected directly into the heart. Rats were perfused with 500 mL oxygenated DMEM (Sigma D-8900) and 1 L of 4% formaldehyde in 0.1 M phosphate buffer. The brains were removed and post-fixed in 4% formaldehyde in 0.1 M phosphate buffer for 7 days on a shaker at room

temperature. A rodent brain matrix (RBM400-C, ASI Instruments, Warren, MI) was used to isolate the brainstem, which was then sectioned into 150 μm slices using a Vibratome (Leica VT100S, Buffalo Grove, IL). Endogenous peroxidases were blocked using methanol peroxide before incubation of slices in 1:250 ExtrAvidin-Peroxidase (Sigma E2886) in 10% normal horse serum immunobuffer, on a shaker at room temperature for 3 days. Labeled neurons were revealed using a nickel-intensified diaminobenzidine reaction, similar to that described by Llewellyn-Smith et al 2005 (Llewellyn-Smith, et al., 2005). Slices containing labeled neurons were embedded in Durcopan resin similar to that described in Llewellyn-Smith and Gnanamanickam (Llewellyn-Smith and Gnanamanickam, 2011). Briefly, slices were dehydrated using graded acetone solutions and then 100% propylene oxide. Slices were incubated in a 1:1 mixture of propylene oxide and Durcopan resin (Sigma) for 1-2 hours before overnight infiltration with undiluted Durcopan. Slices were then mounted on glass slides under coverslips made from Aclar (ProSciTech, Thuringowa, Queensland, Australia) before the resin was polymerized at 60°C for 48 hours. Neurons were digitally reconstructed using an Olympus BH2 microscope and Neurolucida software (version 11, MBF Bioscience, Williston, VT).

***Data acquisition and analyses***

Analog signals were filtered and amplified (extracellular 300 Hz - 3 kHz, 2000x; SSNA 30 Hz - 3 kHz, 20,000x) via Grass Technologies P511AC amplifiers. All signals were recorded using a PowerLab 8SP digitizer and LabChart 6 (ADInstruments, Colorado Springs, CO). SSNA was rectified, integrated, and averaged using a time constant of 28 ms, and is reported as millivolts·seconds (mV·s). Background noise was determined either following ganglionic blockade (30 mg/kg hexamethonium bromide, 1

mg/kg atropine sulfate via i.v.) or post-mortem values and subtracted from nerve activity. Data were obtained in 2 second moving averages during drug administration and compared to baseline values (10 second averages obtained immediately prior to drug administration) as shown in Figure 3. Data points were used to construct 4-parameter baroreflex curves for each animal using SigmaPlot 10.0. Curve parameters were used to create group means and compared between groups by unpaired t-tests. Data were considered statistically significant if p values were less than 0.05. All data are expressed as mean ± standard error of the mean.

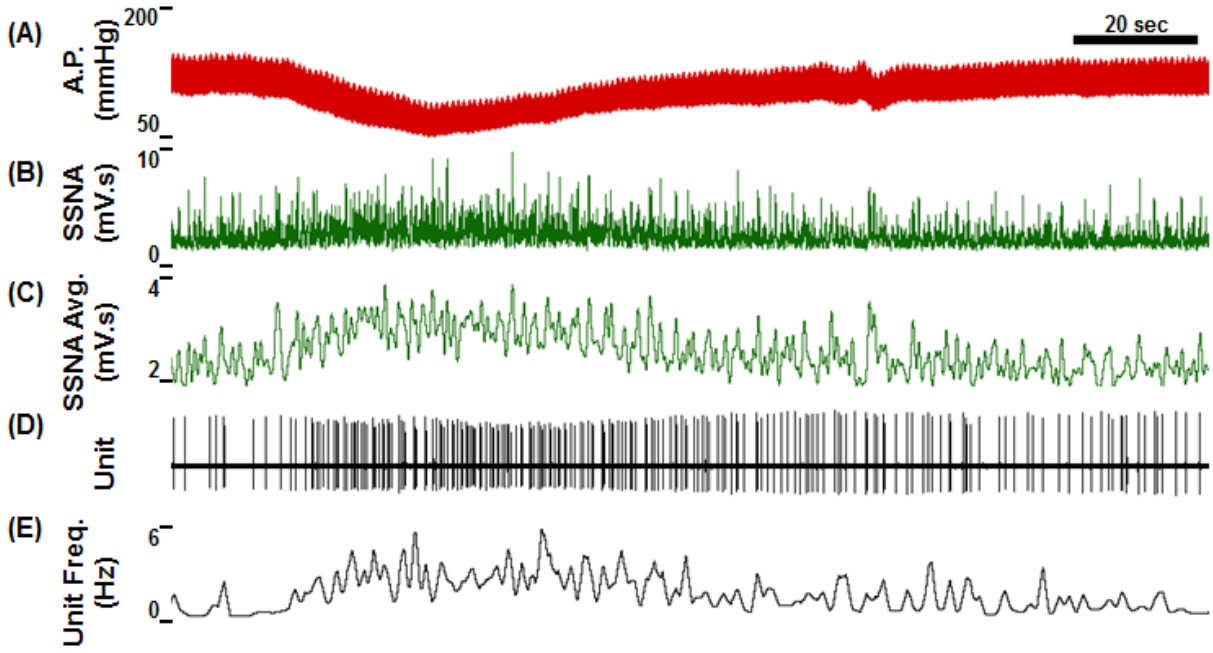


**Figure 3. Individual examples of arterial pressure and splanchnic nerve activity recordings, and extracellular recording of an individual neuron.** (A) Arterial pressure is decreased during i.v. infusion of 1 mg/ml SNP. A corresponding increase is observed in rectified, integrated SSNA signal (B) and smoothed SSNA (C). (D) Single-unit extracellular recording demonstrates an increase in the number of action potentials during the period where arterial pressure is decreased. (E) 2-second moving averages show the neuron increases action potential frequency before returning to baseline as arterial pressure normalizes. A.P., arterial pressure; SSNA, splanchnic sympathetic nerve activity; SSNA Avg., Averaged integrated SSNA; Unit Freq., unit frequency.

## Results

### *Body weight and arterial pressure*

In physically active animals (n = 10), resting mean arterial pressure measured 99 ± 4 mmHg compared to 102 ± 3 mmHg in sedentary animals (n = 11) (Figure 4). Comparison of these resting arterial pressures by two-tailed t-test did not indicate significant differences between groups (p = 0.57). Resting heart rates obtained at time of experimentation were 329 ± 10 bpm for physically active rats and 341 ± 6 bpm for sedentary animals and were not significantly different between groups (p = 0.318). Body weights obtained immediately prior to surgery showed that sedentary rats were significantly heavier than physically active rats (p < 0.0001, 430 ± 6 g versus 379 ± 6 g, respectively) (Figure 4).

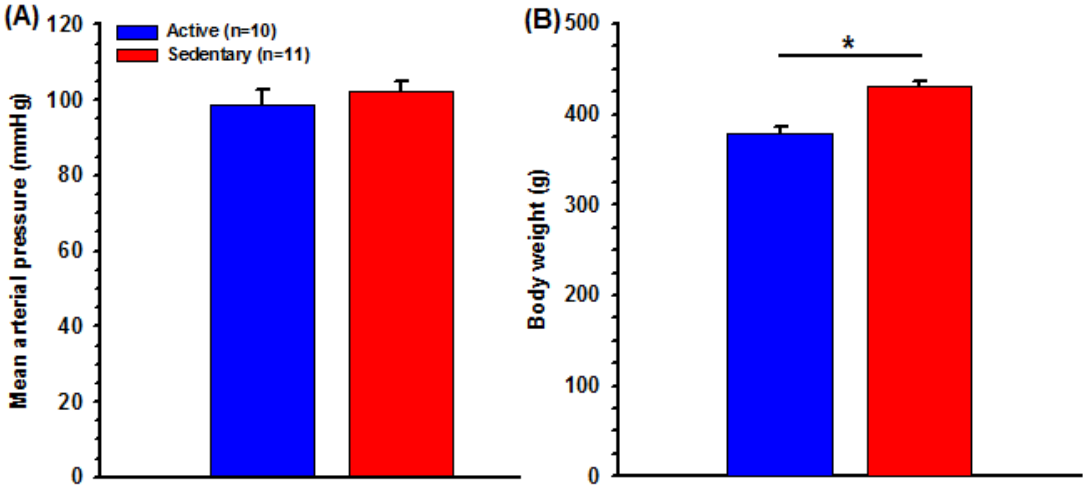


**Figure 4. Resting arterial pressures and body weights at the time of experiments.** (A) Resting arterial pressure was not different between groups in anesthetized rats (p = 0.48). (B) Sedentary rats were significantly heavier than physically active rats on the days of experiments.

### *Barosensitivity of RVLM neurons*

The caudal pole of the facial nucleus was located via the disappearance of field potentials induced by antidromic activation of the facial nerve. Neurons in physically

active animals were located 177 ± 55 µm caudal to the caudal pole of the facial nucleus compared to 132 ± 34 µm caudal to the caudal pole of the facial nucleus in sedentary animals, and the positions of the neurons relative to the caudal pole of the facial nucleus was not significantly different between groups (p = 0.5). The baseline firing frequencies of RVLM neurons were obtained prior to administration of phenylephrine or sodium nitroprusside. Resting firing frequencies measured 3.1 ± 0.6 Hz in physically active versus 2.8 ± 0.6 Hz in sedentary animals and were not significantly different between groups (p = 0.77). Phenylephrine-induced increases in arterial pressure effectively silenced neurons from both groups (Figure 5), producing an average minimum firing frequency that was not significantly different between physically active (0.3 ± 0.2 Hz) versus sedentary (0.02 ± 0.1 Hz) rats (p = 0.26). The maximum increase in firing frequency following nitroprusside-induced decreases in arterial pressure also did not show significant difference between physically active and sedentary animals, measuring 4.4 ± 0.9 Hz in physically active versus 4.0 ± 0.8 Hz in sedentary animals

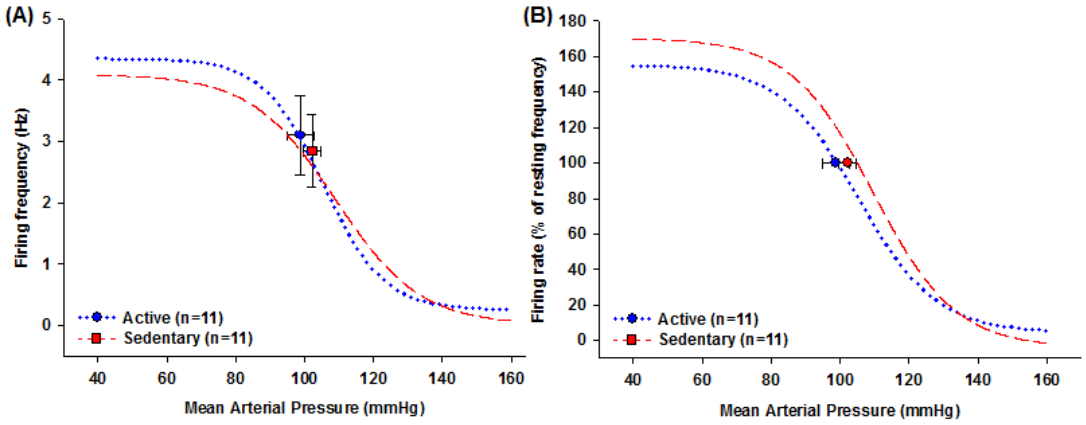


**Figure 5. Baroreflex curves of RVLM neurons.** Barosensitive neurons in the RVLM did not show significant differences in baroreflex curves when examined either by firing frequency (A) or when examined as a percent of resting frequency (B). Curve parameters range, slope, midpoint, and minimum did not show significant differences by either method of analysis. Points on the curves indicate resting values ± S.E.M.

(p=0.83). There were no significant differences in the midpoints (105 ± 4 mmHg in physically active, 109 ± 4 mmHg in sedentary, p = 0.567) or slopes (-8.8 ± 2.0 Hz/mmHg in physically active, -12.2 ± 2.5 Hz/mmHg, p = 0.286) of baroreflex curves between groups. Similar results were observed when examining baroreflex curves as a percent change from the resting firing frequency of neurons. We did not observe significant differences in curve ranges (p = 0.540), slopes (p = 0.907), midpoints (p = 0.488), minimums (p = 0.488), or maximums (p = 0.634) between physically active and sedentary animals.

***Barosensitivity of the splanchnic sympathetic nerve***

Baseline measurements of SSNA were obtained prior to administration of phenylephrine or sodium nitroprusside. We did not find evidence of significant differences in baseline measurements of SSNA in anesthetized physically active versus sedentary rats, in contrast to our previous studies (Mischel and Mueller, 2011; Subramanian and Mueller, 2016). Resting SSNA measured 0.94 ± 0.21 mV.s in physically active versus 0.92 ± 0.19 mV.s in sedentary animals and was not significantly different between groups (p = 0.950). Phenylephrine-induced increases in arterial pressure effectively silenced the splanchnic nerve, producing an average minimum SSNA that was not significantly different between groups (-0.02 ± 0.05 mV·s in physically active animals, 0.07 ± 0.07 mV·s in sedentary animals, p = 0.286) (Figure 6). The maximum increase in SSNA (as a percent of resting value) following nitroprusside-induced decreases in arterial pressu re also did not show significant difference between physically active and sedentary animals, measuring 152 ± 13% in physically active versus 142 ± 11% in sedentary animals (p = 0.596). Furthermore, when examining baroreflex curve parameters in voltage or as a percent change from resting voltage, we

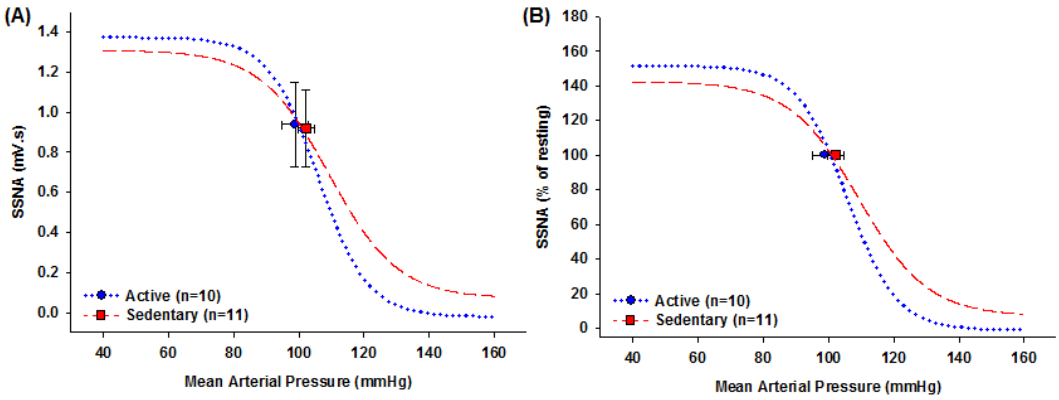


**Figure 6. Baroreflex curves of splanchnic nerves.** Splanchnic nerves did not show significant differences in baroreflex curves when examined either by absolute voltage (A) or when examined as a percent of resting voltage (B). Curve parameters range, slope, midpoint, and minimum did not show significant differences by either method of analysis. Points on the curves indicate resting values ± S.E.M.

did not find significant differences in slopes ($p = 0.116$, $p = 0.116$, respectively), midpoints ($p = 0.383$, $p = 0.372$), or ranges ($p = 0.678$, $p = 0.498$) between sedentary and physically active animals.

### *Morphology of labeled neurons*

Neurons from sedentary (n = 4) and physically active (n = 7) rats that were marked by juxtacellular labeling were reconstructed as shown in Figure 7. Comparison

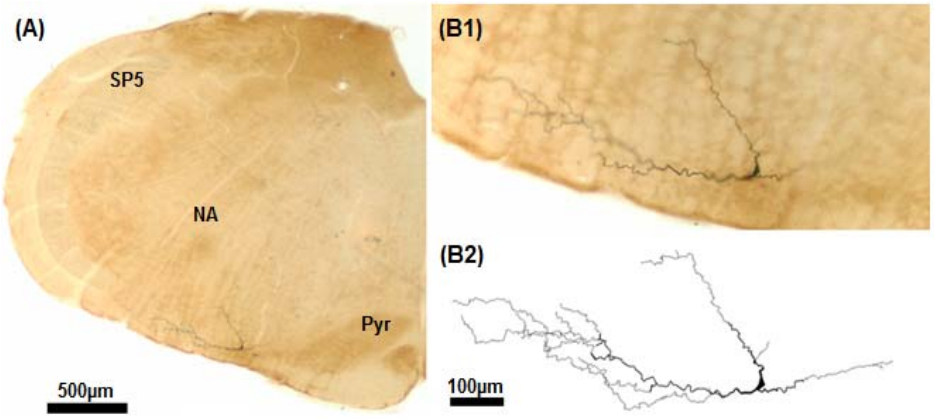


**Figure 7. Example of a neuron juxtacellularly labeled and reconstructed.** (A) Bright-field imaging of brain section obtained from a sedentary animal shows the labeled neuron was found in a region consistent with the RVLM. (B1) Enlarged view of the portion of the labeled neuron located in one 150 µm slice. (B2) The reconstructed neuron, including dendrites found in other slices. Pyr = pyramidal tract; NA = nucleus ambiguus; SP5 = spinal trigeminal tract.

of dendritic morphology by Sholl analysis did not show an interaction between animal group (sedentary versus physically active) and dendritic intersections per 10μm shell (two-way repeated measures ANOVA, p = 0.39) or a difference of intersections between groups (p = 0.17) (Figure 8). Similarly, comparison by total dendritic length per shell did

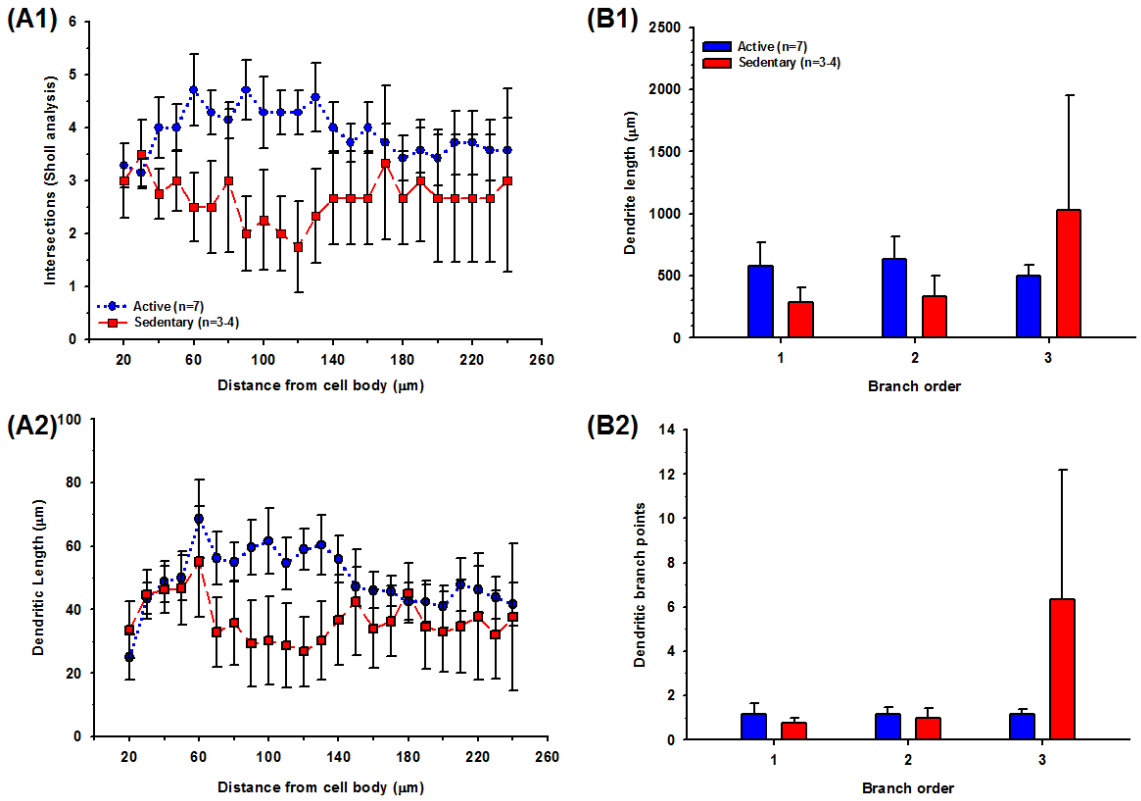


**Figure 8. Comparison of neuronal morphology between sedentary and physically active rats.** Dendritic branching (A1) and dendritic length (A2) were not different between groups when examined by Sholl analysis. Sholl analysis did not indicate significant differences in dendritic branching (A1) or dendritic length (A2) between groups. (B1) Comparison of dendritic length by branch order did not show significant differences between groups, nor did analysis of arborization by branch order (B2). Sedentary animals n = 4 from 20 to 120 μm from cell body by Sholl analysis and for first and second order dendrites, n = 3 after 120 μm and for third order dendrites.

not reveal an interaction between group and dendritic length (p = 0.23) or differences in dendritic length between groups (p = 0.13). The length of dendrites, when examined by branch order, did not reveal an interaction between group and length (p=0.49) and dendritic length by branch order was not significantly different between groups (p=0.48), nor was there an interaction between group and dendritic nodes by branch order

(p=0.265) or a difference between groups in nodes (p = 0.65).

**Discussion**

Previous studies from our group have demonstrated that following exposure to chronic sedentary versus physically active conditions, sedentary rats exhibit greater SSNA in response to nitroprusside-induced decreases in blood pressure than is exhibited by physically active rats. Furthermore, a corresponding difference in SSNA between groups was observed following microinjection of the excitatory amino acid, glutamate, directly into the RVLM (Mischel and Mueller, 2011; Subramanian and Mueller, 2016). These studies suggest that presympathetic RVLM neurons in sedentary rats have functional characteristics which make them more sensitive to sympathoexcitatory stimuli compared to those found in physically active rats. Further supporting the hypothesis that levels of physical activity induce neuroplastic changes among neurons within the RVLM, our group has also reported that the C1 subtype of presympathetic RVLM neurons exhibit significantly greater dendritic arborization and length in sedentary versus physically active rats (Mischel, et al., 2014). Taken together, these studies suggest that presympathetic neurons within the RVLM are an important site of functional and morphological neuroplastic changes that occur as a result of sedentary versus physically active conditions. The purposes of this study were to investigate potential differences in the baroreflex characteristics of presympathetic RVLM neurons, and to examine their correlation to neuronal morphology and baroreflex characteristics of SSNA in sedentary and physically active rats. To do this, we used splanchnic nerve recording and single-unit extracellular recording of RVLM neurons to quantify their responses following pharmacologically-induced changes in blood pressure. Furthermore, we performed juxtacellular labeling on a subset of these

barosensitive neurons in order to reconstruct and examine neurons for differences in morphology between groups. We hypothesized that RVLM neurons in sedentary rats would exhibit an enhanced resting frequency of action potentials, consistent with an increase in sympathetic outflow, compared to physically active rats. We further hypothesized that individually characterized barosensitive RVLM neurons would exhibit enhanced dendritic arborization in sedentary animals, similar to that which was observed in our previous study that examined spinally projecting C1 neurons.

In this study we report that rats living under 10-15 weeks of sedentary conditions weighed significantly more than rats that lived for 12-15 weeks under physically active conditions (spontaneous wheel running). These data align well with previous studies from our group demonstrating increased body weight of sedentary versus physically active rats using a similar model (Mischel, et al., 2014; Mueller and Mischel, 2012; Mischel and Mueller, 2011). Using the findings of Mischel and Mueller 2011 as a basis for our expected effect size, we determine the power of this study on resting nerve activity to be greater than 0.9. One notable difference between this study and previous studies from our group is that in general, the previous studies have reported that sedentary rats also exhibit an increased level of resting SSNA compared to physically active counterparts (Subramanian and Mueller, 2016). In the current study, resting SSNA was not found to be different between sedentary and physically active rats as it was in the previous studies. For example, in Subramanian and Mueller (2016) resting SSNA was 1.15 ± 0.12 mVs in sedentary animals versus 0.48 ± 0.15 mVs in physically active animals, compared to 0.92 ± 0.19 mVs in sedentary animals versus 0.94 ± 0.21 mVs in physically active animals in this study. We also did not find differences between groups when examining resting MAP in this study. However, resting MAP alone is not

an indicator of the effects of sedentary versus physically active conditions as previous studies from our group using similar models have reported both significant differences (Mischel and Mueller, 2011), and no differences in resting MAP between groups (Subramanian and Mueller, 2016). Finally, we did not observe a difference in resting frequency of barosensitive RVLM neurons between groups. The results of this study indicate that in these anesthetized animals, sedentary versus physically active conditions did not result in differences between resting levels of RVLM neuronal activity or SSNA, and did not result in differences in MAP that have previously been observed.

Due to the fact that differences in SNA voltage that can occur due to technical rather than physiological reasons (e.g., differences in contact between electrode and the nerve) there is some debate as to whether SNA can be expressed in terms of voltage or should be normalized to some other metric such as resting or maximum levels (Guild, et al., 2010). Each of these methods is useful for measuring different aspects of the baroreflex, however each have their own drawbacks. For example, normalizing to maximum SNA is unable to demonstrate differences in maximum SNA that occur due to experimental variables, while, results of normalization to resting levels of SNA may be confounded if resting SNA is greatly altered by experimental variables. In fact, studies have shown that analyzing the same data by different methods can indicate significant differences between experimental groups using one method, but not the other (Moffitt, et al., 1998; Head and Burke, 2001). Such studies demonstrate the value of analyzing data by more than one method.

In order to compare data between groups in absolute and relative terms, we have presented our SSNA baroreflex curves in both voltage as well as normalized to resting values in this study. We did not observe differences between sedentary and physically

active rats in either absolute or relative measures of SSNA baroreflex characteristics, as was observed in Mischel and Mueller 2011. However, it should be noted that while the power of these studies to detect differences in maximum SSNA in terms of absolute voltage is greater than 0.9, there was insufficient power to detect differences in maximum SSNA as a percent of resting values due to a high level of variability. While these data did not support the hypothesis we based on our previous studies, there are important differences between studies which could account for the seeming discrepancies. One difference is that in this study there were additional surgical procedures performed on the animal compared to the previous studies, e.g. exposing and electrically stimulating the facial nerve, spinal laminectomy and electrically stimulating the IML. It is possible that these additional procedures could cause changes in SSNA, and neuronal activity, during the experiment that would make demonstration of differences between groups difficult or impossible. Furthermore, it has been reported that noxious stimuli that are generally not sufficient to result in increases in SSNA in anesthetized animals can indeed be made to increase SSNA by disruption of GABAergic inhibition (Muller-Ribeiro, et al., 2014). Therefore, we propose that given the level of physical invasiveness of our experiments, SSNA may have been affected by the level of anesthesia required to maintain an adequate anesthetic depth (i.e., lack of paw withdrawal and lack of increase in arterial pressure following toe-pinch assessment).

Another potential reason for the differences between this study and our previous study, which showed sedentary rats exhibited both a greater resting level of SSNA and an enhanced level of SSNA in response to SNP-induced decreases in arterial pressure, is that there was a slight difference in rat model. In the previous study, experiments

were performed on rats following 10-12 weeks of sedentary versus physically active conditions (Mischel and Mueller, 2011; Subramanian and Mueller, 2016). In contrast, the physically active rats in the present study were under those conditions for 12-15 weeks. While it is true that the SSNA in these animals could be affected by the general increase in nerve activity that occurs with age in multiple models and species (Hart, et al., 2012; Ito, et al., 1986; Kenney, 2010), it should also be noted that in this study, physically active rats changed their daily level of running wheel activity over time. Rats increased their daily running wheel activity, both in terms of time and distance, increasing to a peak at 6 weeks ($p < 0.01$) and significantly decreased activity thereafter ($p < 0.05$) (Figure 9). This decrease in physical activity among older rats may result in

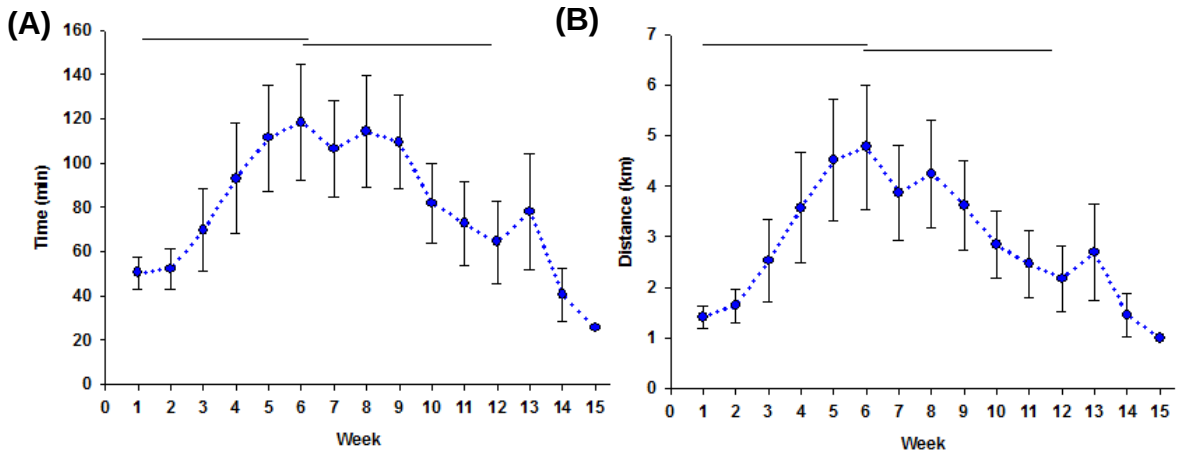


**Figure 9. Average daily wheel activity of physically active rats.** Averages of daily activity over the course of each week was calculated (A) Daily running time increased from week 1 to week 6 before decreasing again through week 12. (B). Daily running distance significantly increased from week 1 to week 6 before decreasing again through week 12. n = 10 from week 1-12, n = 8 at week 13, n = 3 at week 14, n = 2 at week 15.

the physically active rats in this study exhibiting characteristics that more closely resemble the younger sedentary rats from our previous studies (Southerland, et al., 2007; Mischel and Mueller, 2011). In support of this proposed explanation, a recently published study from our group, which examined rats exposed to 12-15 weeks of

sedentary versus physically active conditions, also did not find significant differences in resting SSNA (Dombrowski and Mueller, 2017).

Similar to SSNA, data can be reported in a number of ways to reveal different aspects of neuronal activity. As different subtypes of RVLM neurons are known to have different resting frequencies and may respond to different stimuli, groups often report their findings in more than one way, e.g., in terms of absolute firing frequency and normalized to another measure such as resting frequency (Schreihofer and Guyenet, 2000a; How, et al., 2014). Here, unit activity was presented both in terms of absolute firing frequency in Hz and as a percent of resting frequency, allowing for absolute and relative comparisons between neurons within and between groups. Due to the paucity of published data on extracellular recordings of RVLM neurons in sedentary versus physically active rats, the expected effects of sedentary versus physically active conditions on the activity of RVLM neurons were based primarily on the results published in Kajekar et al 2002 regarding the activity of RVLM neurons during post-exercise hypertension, and Xu et al 2012 regarding RVLM-projecting PVN neurons in a rat model of chronic heart failure. We calculated our statistical power (greater than 0.8) to be sufficient for resting frequency and for maximum frequency and range (absolute and as a percent increase over resting), but insufficient for slope and minimum firing frequency (percent decrease from resting) due to high variability caused by incomplete inhibition. In this study, we did not observe differences between sedentary and physically active rats in either absolute or relative measures of baroreflex characteristics. While these data did not support our initial hypothesis, they are similar to some other studies that examined other risk factors of CVD. For example, Pedrino et al. reported that they were unable to find differences in resting or maximum discharge

frequency between normotensive rats and hypertensive rats fed a high salt diet and administered Angiotensin II (Pedrino, et al., 2013). Similarly, How and colleagues did not find differences in resting activity of barosensitive RVLM neurons between control rats and rats fed high-fat diets. However, they were able to demonstrate that the neurons from obesity prone rats fed high fat diets were resistant to inhibition via administration of cholecystokinin, but RVLM neurons in obesity resistant rats fed high fat diets were not significantly different from neurons in control rats (How, et al., 2014). In contrast, in this study we did not observe significant differences in sensitivity to inhibitory stimuli, which would have been reflected as differences in the slope and minimum of the baroreflex curve. Based on these results, we conclude that in these anesthetized animals, 10-15 weeks of sedentary versus physically active conditions did not result in differences in baroreflex curve parameters.

In contrast to a previous structural study from our group which demonstrated enhanced dendritic length and arborization among presympathetic neurons in the RVLM of sedentary versus physically active rats, we did not find significant differences in neuronal morphology between groups in this study. The primary reason for the discrepancy in results between the previous study and this one is likely due to the small number of juxtacellularly labeled neurons able to be analyzed in the current study. As one of the goals of this study was to record and label neurons concomitantly with recording the ipsilateral splanchnic nerve, we were only able to successfully label and reconstruct seven neurons in physically active animals and four in sedentary animals. This is in stark contrast to the 382 neurons in sedentary rats and 441 neurons from physically active rats which were able to be retrogradely labeled from the T10 level of the IML (Mischel, et al., 2014). Clearly, the two studies should not be compared directly

without first understanding their differences. One of these differences is that the different approaches used may have examined different subsets of neurons. The previous study examined RVLM neurons of the C1 type which were retrograde labeled via spinal cord injections into the IML at T9/T10, the level of the spinal cord consistent with splanchnic sympathetic preganglionic neurons. One theory suggests that C1 neurons, with their tonic low frequency of action potentials, are recruited on an as-needed basis and thus show enhanced markers of neuronal activation compared to non-C1 neurons following sympathoexcitatory stimuli (Burke, et al., 2011; Chan and Sawchenko, 1994; Guyenet, et al., 2013). Based on that theory, our previous study may have included some proportion of quiescent neurons in physically active animals, which would presumably have the least amount of arborization, given the relationship between sedentary conditions and enhanced dendritic arborization (Mischel, et al., 2014). In contrast, the current study was limited in that it only examined neurons that were found due to their spontaneous *in vivo* activity. It is possible that the techniques used in this study created a bias toward locating the most active neurons, and that these neurons may not faithfully represent the morphology of neurons that are less tonically active.

Another possible explanation for the difference in results between our studies is that, while this study included only slow-firing RVLM neurons, which are known to be consistent with C1 neurons, they were not confirmed to be C1 neurons by immunohistochemical means (Brown and Guyenet, 1985; Brown and Guyenet, 1984; Schreihofer and Guyenet, 1997). By not confirming that the neurons in this study were indeed spinally projecting C1 neurons, it is possible that some of the neurons in this study were slower-firing non-C1 neurons. However, it is very unlikely that a proposed

slow-firing non-C1 neuron could be involved for three reasons. Firstly, studies combining *in vivo* recording and immunohistochemical identification have demonstrated the existence of both slow- and fast-firing C1 neurons, but not slow-firing non-C1 neurons (Schreihofer and Guyenet, 1997). Secondly, selective lesioning of C1 neurons has been shown to eliminate the vast majority of slow-firing RVLM neurons and leave primarily fast-firing non-C1 neurons intact (Schreihofer, et al., 2000; Guyenet, et al., 2001). Thirdly, studies have also shown that in bulbospinal RVLM neurons there is a relationship between firing frequency and conduction velocity, with slow-firing C1 neurons also exhibiting low conduction velocities, another characteristic of C1 neurons (Schreihofer and Guyenet, 1997; Schreihofer and Guyenet, 2000a). Taken together, these studies would suggest that by labeling and reconstructing slow-firing barosensitive neurons in this study we were, in effect, selecting for a subset of C1 neurons.

**Technical limitations**

One technical limitation of this study on sedentary versus physically active rat is the basic assumption that all sedentary rats are equally sedentary. Sedentary animals are considered sedentary because of the lack of a running wheel or other means to engage in physically activity. However, no data were obtained in the present study on how little, or how much, they move within their home cage. Future studies such as this one would benefit from monitoring movement of rats within their cages, e.g., via infrared beams or sensors to detect changes in pressure on the cage floor, which could measure the extent of locomotor activity among sedentary rats, despite the presence of a running wheel. Similarly, this study assumes that all physical activity of rats occurs via the in-cage running wheel, but makes the additional assumption that different levels

of physical activity do not result in different levels of SNA or different levels of activity among RVLM neurons. Ideally, experiments would be performed in a way that allowed for differences in levels of physical activity. For example, rats with low running distances prior to experiments could be tested as a different group from rats with high running distances, and sedentary rats that were relatively active would be tested separately from sedentary animals with the least amount of in-cage movement. However, as variability in RVLM and nerve activity can vary greatly between individual animals, testing animals in multiple additional groups could complicate performing and interpreting such a study.

Indeed, variability between individuals has been shown to make comparisons of SNA difficult, as it is sometimes poorly correlated with arterial pressure (Charkoudian, 2010;Hart, et al., 2012). In this study, we based our number of animals on previous studies from our group and others using related models (Huang, et al., 2006; Mischel and Mueller, 2011; Schreihofer, et al., 2007; Miki, et al., 2003). However, our variability in the range of splanchnic nerve responses, and the corresponding variability in slope, primarily as a percent of resting values, make this study somewhat under powered compared to our initial estimates. It is for this reason that we are unable to firmly conclude that 10-15 weeks of sedentary versus physically conditions do not result in differences in baroreflex characteristics of the splanchnic nerve, but rather that we did not observe them in these animals. Similarly, our prediction of sample size for RVLM unit activity was based on models generally related to control of autonomic function because little is currently known about the long term effects of sedentary versus physically active conditions on RVLM neurons (Kajekar, et al., 2002; Almado, et al., 2014; Xu, et al., 2012; Pedrino, et al., 2013; How, et al., 2014). In this case, the

variability of the minimum activity of neurons during inhibition (e.g., incomplete inhibition despite strong increases in arterial pressure), and the corresponding slope, when expressed as a percent of resting values causes our study to be underpowered for those parameters.

Another limitation in this study is the small number of neurons characterized and labeled. As the brainstem is subject to movement as a result of respiratory activity, it is sometimes difficult to maintain stable recordings for long enough both to obtain full baroreflex curves for neurons and to perform juxtacellular labeling for reconstruction. This difficulty is compounded by the fact that altering blood pressure can also cause changes in the quality of neuronal recordings, presumably due to pressure-induced changes in brainstem tissue (i.e., changes in arterial pressure can cause pulsations in tissue, altering the distance between the neuron and the electrode) (Humphrey and Schmidt, 1990). Presumably, this effect caused some neurons to become damaged or lost before they could be labeled. Furthermore, as dendrites can extend hundreds of microns from the cell body, covering large portions of the RVLM, it is generally advised that only one neuron per side of the brainstem is labeled in order to avoid ambiguity (Schreihofer and Guyenet, 1997; Mandel and Schreihofer, 2006).

**Perspectives**

Previous studies from our group have reported differences in functional, morphological, and molecular changes within the RVLM, a region of the brainstem that contributes to SNA, in rats exposed to sedentary versus physically active conditions (Mischel and Mueller, 2011; Mueller and Mischel, 2012; Mischel, et al., 2014; Subramanian and Mueller, 2016). These studies have also reported corresponding differences in SSNA, which are assumed to be a result of the neuroplasticity which

occurs in the RVLM. In this study we were unable to support the hypothesis that differences in levels of physical activity result in changes to the characteristics of barosensitive neurons that are presumed to contribute to SSNA. This lack of support for our hypothesis should be viewed critically in light of two key facts. First, this study only examines spontaneously-active, slow-firing, barosensitive neurons in the RVLM, consistent with the C1 subtype, which are only one of at least three types of neurons known to contribute SNA (Brown and Guyenet, 1984; Brown and Guyenet, 1985; Schreihofer and Guyenet, 1997). Second, selective lesioning of C1 neurons does not eliminate the ability of the RVLM to regulate to SNA (Schreihofer, et al., 2000; Madden, et al., 1999), indicating that other types of neurons located in the RVLM may also play a role in the differences in SSNA our group previously reported as a result of sedentary versus physically active conditions. Third, the RVLM is only one of multiple presympathetic regions that are known to contribute to regulation of SNA (Strack, et al., 1989; Krout, et al., 2005; Chen and Toney, 2010). Therefore it is possible that some or all of these other regions may also contribute to changes in SNA that occur as a result of exposure to risk factors for CVD, such as sedentary conditions (Beatty, et al., 2005; DiCarlo and Bishop, 1988; Chen and Toney, 2003). Chapter 3 of this dissertation examines the use of a technique, manganese enhanced magnetic resonance imaging, which may be useful in future studies to examine neuronal activity, *in vivo,* in the RVLM as well as other regions of the brain involved in control of autonomic function.

# CHAPTER 3 - EVALUATION OF NEURONAL ACTIVITY WITHIN THE RVLM OF SEDENTARY AND PHYSICALLY ACTIVE RATS USING MANGANESE ENHANCED MAGNETIC RESONANCE IMAGING

## Introduction

Elevated sympathetic nerve activity (SNA) has been implicated in the development and progression of cardiovascular disease (CVD), the leading cause of death among American adults (Malpas, 2010; Mendis, et al., 2014). While SNA itself is subject to influence by multiple factors, it is primarily regulated by the activity of neurons within a region of the brainstem known as the rostral ventrolateral medulla (RVLM) (Ross, et al., 1984b). The RVLM is a bilateral structure which contains neurons that project to the intermediolateral cell column of the spinal cord and release glutamate on to sympathetic preganglionic neurons to increase SNA (McAllen, et al., 1994; Dampney, 1994; Jansen, et al., 1995; Agarwal and Calaresu, 1991; Oshima, et al., 2006). By integrating excitatory and inhibitory signals from other regions of the brain, many of the neurons of the RVLM are tonically active and their rate of activity is able to be bidirectionally modulated, resulting in increased or decreased SNA, according to physiological demand (Guyenet, 2006; Brown and Guyenet, 1985; Schreihofer and Guyenet, 2002).

A large body of literature exists which shows a correlation between elevated SNA in humans and CVD-related conditions (Charkoudian and Rabbitts, 2009). For instance, individuals with hypertension have been shown to have increased levels of SNA, with greater increases reported in male and aged individuals, compared to their female and younger counterparts, respectively (Hart, et al., 2012). Individuals suffering from obstructive sleep apnea, another risk factor for CVD, have been shown to exhibit persistent daytime increases in SNA and arterial pressure compared to individuals who

do not experience apneic events while asleep (Narkiewicz and Somers, 1997). Similarly, there is evidence to suggest that there may be differences in SNA among sedentary and physically active individuals (Senitko, et al., 2002). Senitko et al. demonstrated that the transient hypotension seen following exercise is due to different causes between sedentary and physically active individuals (Senitko, et al., 2002). They showed that in sedentary individuals, post-exercise hypotension is primarily due to increased vasodilation (presumably through a reduction in sympathetic tone), whereas it was primarily due to a reduction in cardiac output in endurance trained individuals. However, previous human studies directly examining the effect of exercise on muscle SNA of the peroneal nerve have had difficulty demonstrating a statistically significant correlation between a sedentary lifestyle and increases in SNA, possibly due to insufficient statistical power as a result of inter-individual variability (Ray and Carter, 2010; Delaney, et al., 2010; Charkoudian, 2010).

In contrast to the technical limitations inherent to recording some forms of SNA in human subjects (e.g., the invasiveness of simultaneously recording multiple sympathetic nerves), studies taking advantage of animal models have been better able to explore the connection between physically active versus sedentary conditions and changes in SNA. Previous studies from our laboratory have been able to demonstrate significantly higher resting splanchnic SNA (SSNA) in chronically sedentary rats compared to physically active (spontaneous wheel-running) controls (Mischel and Mueller, 2011). In addition to this increased resting SSNA, there was also a significantly enhanced increase in SSNA observed in sedentary versus physically active rats following a sympathoexcitatory stimulus (a decrease in arterial pressure following i.v. infusion of sodium nitroprusside). This animal study offered another key benefit to

understanding the potential mechanisms behind the increased SSNA in sedentary rats; the ability to use microinjections of the excitatory amino acid, glutamate, to measure SSNA following direct activation of sympathoexcitatory neurons located within the RVLM. Using these microinjections, our group was able to demonstrate that sedentary rats exhibited greater increases in SSNA than was seen in physically active rats, suggesting that compared to physically active conditions, sedentary conditions lead to enhanced sensitivity of the RVLM to sympathoexcitatory stimuli, and a corresponding increase in SNA.

Traditional techniques for identifying potential differences in neuronal activity that may contribute to dysregulation of SNA, such as FOS studies or electrophysiology, are generally cross-sectional and only examine each animal at one time point. While such techniques can demonstrate potential differences in neuronal activity at a given time point, their cross-sectional designs would be unable to identify within-subject changes in neuronal activity due to chronic exposure to sedentary versus physically active conditions. Furthermore, the neuronal activities in an anesthetized animal during sacrifice for a FOS study or while performing an electrophysiology study may not accurately reflect the activity that occurs under 'awake' conditions (Dorward, et al., 1985; Takayama, et al., 1994). One way to explore the question of whether sedentary versus physically active conditions result in different levels of neuronal activity within the RVLM would be to use a longitudinal method which can evaluate *in vivo* neuronal activity, in awake subjects, both before and after exposure to those conditions.

One technique, manganese enhanced magnetic resonance imaging (MEMRI), has emerged as a way to evaluate how experimental variables affect neuronal activity, *in vivo*, over multiple trials (Van der Linden, et al., 2002; Inoue, et al., 2011; Jung, et al.,

2014; Eschenko, et al., 2012). MEMRI is a form of MRI which uses manganese as a contrast agent to identify regions within the brain that have increased neuronal activity (Malheiros, et al., 2015; Lin and Koretsky, 1997). In its divalent form, manganese ($Mn^{2+}$) is a paramagnetic ion that is able to decrease the T1 relaxation time constant of protons (Mendonca-Dias, et al., 1983; Geraldes, et al., 1986). When images are acquired with short repetition times (T1 weighted imaging), the decrease in T1 effectively causes an increase in the signal intensity in regions with greater concentrations of $Mn^{2+}$. Because $Mn^{2+}$ has ionic characteristics similar to those of divalent calcium, which is used by neurons for release of neurotransmitters, it is able to enter active neurons primarily via L-type voltage-gated calcium channels during action potentials (Wang, et al., 2015; Nasu, et al., 1995; Ulyanova, et al., 2017). Due to this activity-dependent uptake into neurons and a slow rate of efflux, $Mn^{2+}$ accumulates in regions of the brain with tonic or stimulated levels of neuronal activity (Lin and Koretsky, 1997; Kuo, et al., 2006). Following systemic administration of $Mn^{2+}$ (e.g., via i.p. injection), it is absorbed via the portal veins, distributed throughout the body, and enters the cerebrospinal fluid (CSF) via the choroid plexus and regions lacking a blood brain barrier (Chuang and Koretsky, 2009; Greenberg, et al., 1943). Once in the CSF, $Mn^{2+}$ is taken up by active neurons in the awake, behaving animal subject. Previous studies have shown that $Mn^{2+}$ is cleared from the blood and CSF within approximately 24 hours of systemic administration, with the peak increase in brain signal intensity in many regions generally occurring in approximately the same amount of time (Lee, et al., 2005; Zheng, et al., 2000; Aoki, et al., 2004). When $Mn^{2+}$ is administered at non-saturating, non-toxic doses, the increased signal intensity returns to baseline levels over the course of 2 to 3 weeks, meaning that assessments of neuronal activity via MEMRI can be

performed hours or days after the initial administration of manganese, and will reflect the level of neuronal activity which occurred during the approximately 24 hour period of uptake (Van der Linden, et al., 2002; Chuang, et al., 2009). Furthermore, because signal intensities eventually return to baseline levels, MEMRI offers the potential to longitudinally assess neuronal activity in the same animal subjects both before and after the introduction of an experimental variable.

In this study we used MEMRI to longitudinally evaluate the effects of sedentary versus physically active conditions on neuronal activity within the RVLM in a rat model. We evaluated neuronal activity in the RVLM by measuring activity-dependent increases in signal intensity both before and after exposure to 12 weeks of sedentary versus physically active conditions. By using intraperitoneal (i.p.) administration of $Mn^{2+}$ and MEMRI, we probed for the development of differential increases in neuronal activity, indicated by differential increases in signal intensity compared to baseline (non-injected) imaging sessions, in sedentary and physically active rats. Based on previously reported increases in SSNA in sedentary rats, we hypothesized that sedentary animals would show enhanced neuronal activity within the RVLM, as indicated by an enhanced increase in signal intensity compared to physically active control animals.

## Methods

### *Ethical statement*

All protocols were approved by IACUC of Wayne State University and performed according to the guidelines published by the NIH and in the American Physiological Society's *Guiding Principles in the Care and Use of Animals.*

### *Animal model and systemic injections of $Mn^{2+}$*

4-week old male Sprague Dawley rats (Harlan, Indianapolis, IN) were singly

housed in polycarbonate cages upon arrival (n = 21, weight 92 ± 1 g) under controlled temperature and light (12:12 light:dark cycle) conditions. At all times, rats had *ad libitum* access to tap water and food (Purina LabDiet 5001 Purina Mills, Richmond, IN). Figure 10 demonstrates the timeline of procedures in these experiments. After a period of acclimatization, surgery was performed to implant i.p. catheters in all rats. Under

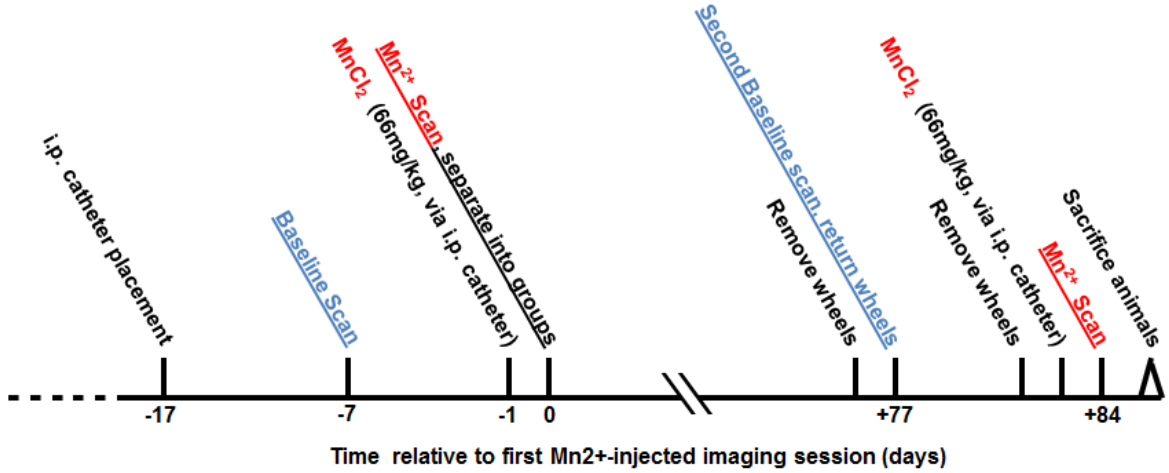


**Figure 10. Timeline of procedures for MEMRI experiments.** Chronic i.p. catheters were placed in animals 10 days prior baseline imaging. Six days later, $Mn^{2+}$ was administered 24 hours before the first MEMRI session. Animals were separated into sedentary and physically active groups for 11 weeks before a new baseline imaging session, and a second MEMRI session at 12 weeks.

isoflurane anesthesia (3% induction followed by 2% maintenance, in 100% $O_2$; Ohio Vaporizer, ASE, Gurnee, IL), the chronic catheters (Braintree Scientific, R-FC-L, Braintree, MA) were placed subcutaneously with the end of the internal segment located inside the i.p. space and the external segment located posteriorly at the base of the neck (150 ± 2 g at surgery). After a minimum of 10 days recovery, the rats (196 ± 3 g) were imaged under acute anesthesia (see below) to establish baseline MRI values of RVLM voxel intensity. Six days following the initial scan, during daylight hours, rats were given $MnCl_2 \cdot 4H_2O$ (66 mg/kg, Sigma Aldrich, St. Louis, MO), prepared in sterile saline, via i.p. catheter. Catheters were flushed with saline in order to ensure complete

delivery of $MnCl_2$. 24 hours following administration of the manganese solution, a new set of images were obtained to assess the uptake of $Mn^{2+}$ which had occurred during the period between administration and imaging. Rats were then randomly assigned to physically active (free access to an in-cage running wheel) or sedentary (no running wheel) groups. A bike computer (SigmaSport, Olney, IL) was used to monitor daily running wheel activity of physically active rats. Rats were maintained under sedentary or physically active conditions until a second set of paired non-injected and injected imaging sessions under acute anesthesia occurred at 11 and 12 weeks, respectively after the initial $Mn^{2+}$ administration. Catheters that had retracted throughout the course of the experiment were replaced under anesthesia 4 days before administration of $MnCl_2$ for the 12 week imaging time point. Data obtained from the second set of images were compared between groups, and to that obtained from the first pair of imaging sessions.

***MRI acquisition***

For each imaging session, rats were anesthetized with isoflurane (5 % induction, 1.5 - 2.25 % maintenance, in room air) and placed on a carriage heated by circulating water inside of a Bruker 7T ClinScan small animal MRI controlled by a Siemens console using Syngo software (Siemens Corporation, Washington D.C., USA). Respiration and heart rate were monitored during imaging with an SA Instruments (Stony Brook, NY) small animal monitoring system. For each scan, the head was stabilized during imaging by a combination of a bite bar assembly that supplied isoflurane, the nose cone, and the surface head coil, which was placed on top of the head and used to obtain signals. Image acquisition was performed using the transmit-only whole body coil and a receive-only surface coil placed over the head and neck region. T1-weighted localizing

sequences were performed to standardize the position of the brains using the pituitary as a landmark. Rats were then imaged via T1 weighted and T1 map imaging techniques (Figure 11). Following imaging, rats were placed on a heating pad maintained at 37°C and allowed to regain consciousness, indicated by sternal recumbency, before being returned to their home cages.

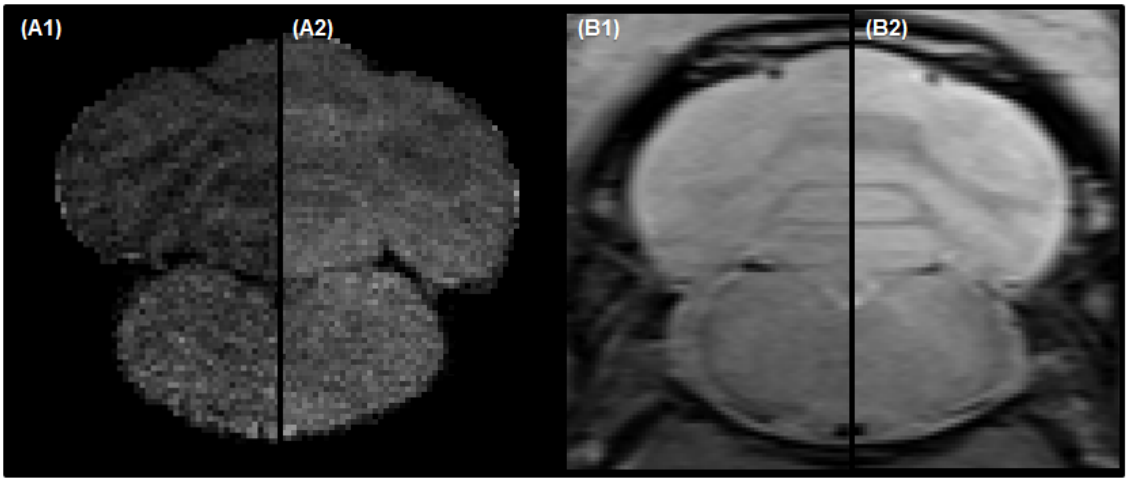


**Figure 11. Examples of imaging before and after administration of manganese.** (A) T1 weighted images as obtained before (A1) and after (A2) administration of manganese. (B) T1 map images as obtained before (B1) and after (B2) administration of manganese via chronic i.p. catheter.

To eliminate potential acute effects of physical activity (Kajekar, et al., 2002; Kulics, et al., 1999), running wheels were removed from cages the day before the imaging session (after 11 weeks of physical activity) and returned following imaging. Similarly, wheels were again removed the day before administration of $Mn^{2+}$ to eliminate potential effects of physical activity on manganese uptake within the RVLM (after 12 weeks of physical activity), and returned following imaging. Rats were sacrificed 24 - 48 hours after the final imaging session by being deeply anesthetized with 100 mg/kg Fatal Plus (Vortech, Dearborn, MI) delivered via i.p. catheter before transcardial perfusion.

The total imaging time per rat was approximately one hour, consisting of 30 minutes for T1 weighted imaging and 2 x 15 minutes for T1 map imaging. To ensure

adequate time for anesthesia, positioning, configuration, and monitored recovery, animals were imaged in the order they were injected, at 90 minute intervals.

***T1 weighted imaging***

T1 weighted imaging was performed similar to that described in Holt *et al*. (Holt, et al., 2010). Two replicates of two separate types of imaging were performed on each animal: magnetization prepared rapid acquisition gradient echo (MPRAGE); and produced proton density weighted (PDGE) images. MPRAGE and PDGE images shared parameters and both produced a series of images representing the entire brain, from the olfactory bulbs to the spinomedullary junction, at a resolution of 130x130 μm along the dorsoventral and mediolateral axes and 260 μm along the rostrocaudal axis. The summed MPRAGE images were divided by the summed PDGE images using R language scripts developed in-house to create T1 weighted images which were free of the effects of B1 field inhomogeneity (Van de Moortele, et al., 2009; Holt, et al., 2010).

***T1 map imaging***

Scanning was performed to quantify two separate rostrocaudal regions of the RVLM. Separate images were obtained of the regions of the brainstem 400 μm immediately caudal to, and rostral to, the caudal pole of the facial nucleus, a traditional landmark for the RVLM. Each region was imaged at 8 repetition times (TR) with an increasing number of observations at shorter TRs to compensate for decreased signal-to-noise ratios (6 x 150 ms, 1 x 3500 ms, 2 x 1000 ms, 1 x 1900 ms, 4 x 350 ms, 1x 2 700 ms, 5 x 250 ms, 3 x 500 ms). Using ImageJ, images with the same TRs were registered (rigid body) and averaged to produce single images for that TR before images were registered across all 8 TRs. Image intensity values in a region of interest (ROIs) were obtained via ImageJ for all TRs and, T1 was calculated by fitting data to a

3-parameter equation using R language scripts developed in-house and the minpack.lm package (v.1.1.1, Timur V. Elzhov and Katharine M. Mullen minpack.lm: R interface to the Levenberg-Marquardt nonlinear least-squares algorithm found in MINPACK. R package version 1.1–1) (Bissig and Berkowitz, 2011).

***Defining RVLM ROIs***

The location of the RVLM was defined anatomically based upon a rat atlas (Paxinos and Watson, 2007) and anatomical studies performed by our laboratory and others (Ross, et al., 1984a; Mischel, et al., 2014; Ruggiero, et al., 1989) (Figure 12). We previously confirmed the RVLM was identifiable in MEMRI by using microinjections of glutamate to functionally identify the RVLM via in vivo increases in arterial pressure,

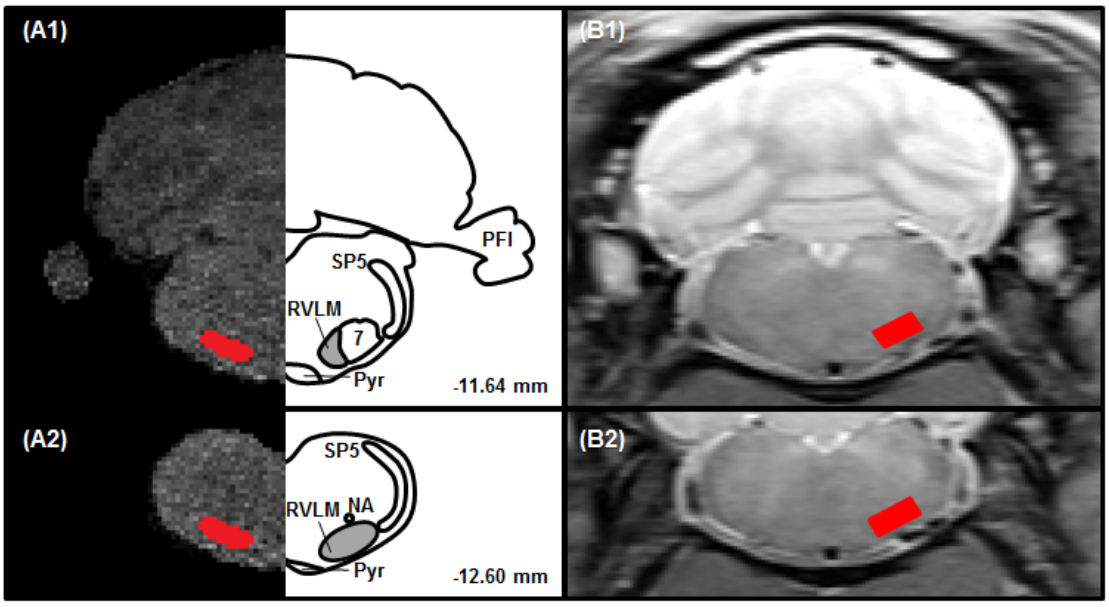


**Figure 12. Location of RVLM on T1 weighted and T1 map magnetic resonance images.** Regions of interest are shown in red. T1 weighted MRI images show the rostral (A1) and caudal (A2) extent of the region analyzed, and corresponding stereotaxic schematics (right panels, modified from Paxinos and Watson, 6th edition). (B) T1 map images of the 400 µm slices corresponding to the rostral (B1) and caudal (B2) RVLM.

followed by post mortem microinjection of manganese at the same stereotaxic coordinates prior to imaging (Huereca, et al., 2017). ROIs were hand drawn on images

in the region consistent with the RVLM. For T1 weighted imaging, ROIs were manually drawn and voxel intensities, measured in arbitrary units (a.u.), were obtained using MRIcro (version 1.40 Chris Rorden. www.mricro.com). ROIs were drawn separately on the left and right RVLM to account for potential physical misalignment of the brain during the imaging session. Left and right ROIs were matched based on their rostrocaudal position relative to the caudal pole of the facial nucleus before their intensities were averaged to obtain mean intensities for each rostrocaudal level of the RVLM. Mean RVLM voxel intensities were obtained for the 520 μm (2 260 μm virtual slices) rostral too, and 520 μm caudal too, the caudal pole of the facial nucleus. For T1 map imaging, ImageJ was used to draw ROIs over areas corresponding to the RVLM. T1 was calculated separately for left and right RVLM then averaged to calculate T1 for rostral and caudal levels of the RVLM. The reciprocal of T1 (1/T1) was used to compare subjects as 1/T1 directly reflects manganese concentrations (Chuang, et al., 2009).

***Statistics***

Data were analyzed using SPSS Version 24 (IBM Corporation) SigmaStat Version 3.5 (Systat Software, San Jose, CA) and SigmaStat Version 3.5 (Systat Software, San Jose, CA). Three-way repeated measures ANOVA tests were used to examine interactions between groups (physically active versus sedentary), the effect of manganese administration (pre- versus post-injection), and time point (before versus after exposure to experimental conditions). Two-way repeated measures ANOVA tests were used to examine interactions between group and time point. A standard two-tailed Student's t-test was used to assess potential differences between groups at individual time points, and within groups between time points. Data were considered statistically

significant if p values were less than 0.05. All data are expressed as mean ± standard error of the mean.

## Results

### *Body weights*

Naïve juvenile rats were randomly separated into groups, to be designated as physically active or sedentary following the week 0 imaging session. There were no significant differences in body weight between groups at time of arrival, implantation of i.p. catheters, initial baseline imaging session (week -1), first administration of manganese, during imaging following the first administration of $MnCl_2$ (week 0), or through the second week of sedentary versus physically active conditions. Beginning at week 4 and continuing through week 11, sedentary rats were significantly heavier than physically active rats ($p = 0.028$). At week 12, during the post-injected imaging session, rats from both groups weighed significantly less than they did at their week 11 imaging session ($p < 0.001$) and weights between groups were no longer significantly different ($p=0.1$) (Figure 13). Animals that underwent catheter replacement surgery between the

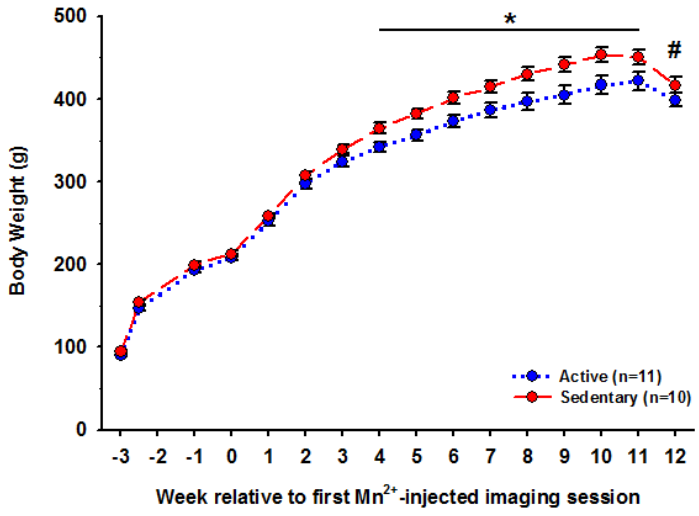


**Figure 13. Body weights of animals throughout MEMRI experiments.** Weights differed between groups after 4 weeks of sedentary versus physically active conditions (*p<0.001). Following Mn2+ administration at week 12, both groups lost a significant amount of weight ($^{\#}p < 0.001$) and weights were no longer different between groups (p=0.10).

week 11 and week 12 imaging sessions were not significantly different compared to

animals of their group that did not have surgery when examined by T1 map or unprocessed T1 weighted values obtained at the week 12 imaging session, or by T1 values expressed as a percent increase over week 11 values (data not shown, $p > 0.1$).

***T1 weighted imaging***

Figure 14 shows the results of T1 weighted imaging at all time points. T1 weighted imaging of the RVLM indicated no significant difference in absolute voxel intensity between groups at week -1 non-injected scans (1625 ± 18 a.u. physically

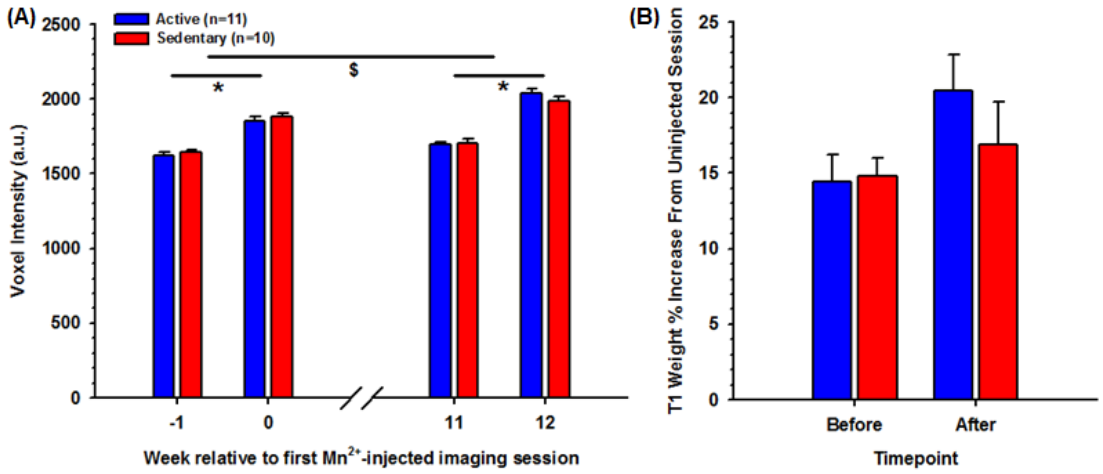


**Figure 14. T1 weighted analysis of RVLM signal intensity before and after 12 weeks of sedentary versus physically active conditions.** (A) Unprocessed T1 weighted values indicate significant increases in voxel intensity following manganese injections at week 0 and week 12 (* $p < 0.001$). It also indicates a main effect of time ($^{\$}$ $p < 0.001$) with an interaction between manganese administration and time ($p = 0.033$) indicating significant increases in signal intensity after sedentary or physically active conditions, but no differences between groups at any point. (B) Analysis of T1 weighted images as a percent change versus the previous non-injected imaging session does not show significant differences between groups ($p = 0.49$) or an effect of time ($p = 0.62$).

active versus 1644 ± 14 a.u. sedentary rats) or at week 0 injected scans (1856 ± 28 a.u. physically active versus 1886 ± 20 a.u. sedentary rats). The i.p. administration of manganese 24 hours prior to the week 0 imaging session caused increases in voxel intensity ($p < 0.001$), measuring 14 ± 2% and 15 ± 1% in physically active and sedentary groups, respectively, in RVLM voxel intensity compared to their baseline

values. No significant differences were observed between groups ($p = 0.84$).

After 11 weeks of physically active versus sedentary conditions, rats were imaged again to establish new baseline values. RVLM voxel intensity values measured 1695 ± 17 a.u. in physically active versus 1707 ± 26 a.u. in sedentary animals, showing a slight but significant increase from their initial baseline values obtained at week -1 ($p = 0.004$). There was no interaction between time point and sedentary versus physically active conditions ($p = 0.862$). At week 12, 24 hours after a second injection of manganese, RVLM voxel intensity values increased significantly ($p < 0.001$), measuring 2037 ± 30 a.u. in physically active versus 1988 ± 28 a.u. in sedentary animals. These values indicate 20 ± 2 % and 17 ± 8 % increases in intensity, respectively, compared to the week 11 baseline values. Animals exhibited a significant increase in unprocessed post-injection RVLM voxel intensity at week 12 versus week 0, indicating a main effect of time ($p < 0.001$). However, we did not observe a significant interaction between time, group, and $Mn^{2+}$ administration in unprocessed RVLM voxel intensities ($p = 0.283$, three-way repeated measures ANOVA) or time and group in unprocessed RVLM voxel intensities from week 11 to week 12 ($p = 0.312$, two-way repeated measures ANOVA) and no interaction between time point and group was found when measured as the unprocessed increase in intensity from week 0 to week 12 ($p = 0.126$). Furthermore, when the post-injected values at weeks 0 and 12 were compared as percent increases from their respective baseline imaging sessions (i.e. the increase from week -1 to week 0 versus from week 11 to week 12), the increase in intensity from week 0 to week 12 became nonsignificant ($p = 0.062$) with no interaction between time and group ($p = 0.341$).

### *T1 map imaging*

Figure 15 shows the results of T1 map imaging at all time points. The results of T1 map imaging were generally similar to those found in T1 weighted imaging. In the week -1 baseline imaging session, 1/T1 values in the RVLM of physically active animals

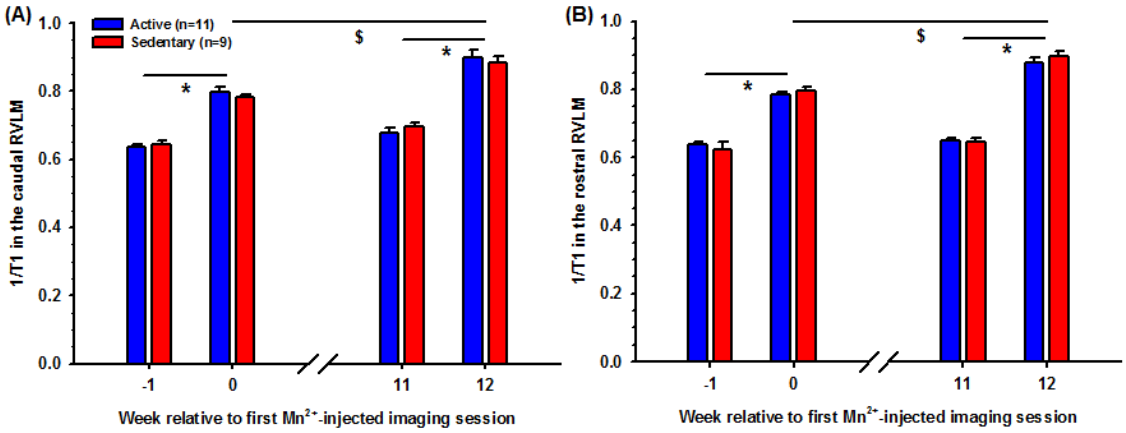


**Figure 15. T1 map analysis of RVLM signal intensity before and after 12 weeks of sedentary versus physically active conditions.** Analysis of the caudal (A) and rostral (B) RVLM indicate a significant increase in 1/T1 following $Mn^{2+}$ administration at weeks 0 and 12 (*$p<0.001$), with significantly greater 1/T1 values at week 12 versus week 0 ($^{\$}p<0.001$). No differences were observed at week 11 versus week -1 ($p=0.30$) or between groups at any time.

were 0.637 ± 0.008 in the caudal section and 0.638 ± 0.007 in the rostral section, compared to 0.644 ± 0.009 in the caudal section and 0.625 ± 0.019 in the rostral section of the RVLM of sedentary animals. 24 hours following i.p. administration of manganese, 1/T1 values in the RVLM of physically active animals had significantly increased to 0.797 ± 0.015 in the caudal section and 0.785 ± 0.007 in the rostral section ($p < 0.001$), compared to 0.782 ± 0.009 in the caudal RVLM and 0.797 ± 0.009 in the rostral of the RVLM of sedentary animals ($p < 0.001$). There were no significant differences in 1/T1 between groups at week -1 or week 0 in either caudal or rostral sections of the RVLM.

After 11 weeks of physically active versus sedentary conditions, 1/T1 values in physically active animals had decreased from their post-injection values at week 0 to

0.679 ± 0.012 in the caudal section and 0.648 ± 0.010 in the rostral section of the RVLM in physically active animals and 0.696 ± 0.011 in the caudal and 0.644 ± 0.012 in the rostral section of the RVLM of sedentary animals. The decrease in 1/T1 was not significantly different between groups ($p = 0.425$) and values at week 11 were not significantly different from values at week -1 ($p= 0 .301$). At week 12, 24 hours after a second injection of manganese, 1/T1 increased to 0.899 ± 0.023 in the caudal section and 0.880 ± 0.013 in the rostral section of the RVLM in physically active animals and 0.885 ± 0.020 in the caudal and 0.899 ± 0.013 in the rostral section of the RVLM of sedentary animals. 1/T1 was significantly increased at week 12 compared to week 11 values in both the rostral and caudal RVLM ($p < 0.001$), but there was no interaction between group and injection at either the rostral ($p = 0.419$) or caudal ($p = 0.376$) level of the RVLM. Again, we observed a slight but significant increase in 1/T1 at week 12 compared to week 0 in sedentary and physically active rats, in both caudal and rostral sections of the RVLM ($p<0.001$). However, we did not observe differences in manganese uptake, as indicated by 1/T1 values, between physically active versus sedentary animals.

***Rostrocaudal analysis by T1 weighted imaging***

Based upon our previous structural study which demonstrated a caudal to rostral gradient of increased dendritic arborization among C1 neurons in sedentary, but not physically active animals (Mischel, et al., 2014), we examined each T1 weighted coronal image of the RVLM for a corresponding increase in signal intensity at the week 12 time point (Figure 16). No interaction was found between group and rostrocaudal position ($p=0.788$, two-way repeated measures ANOVA). No effect of rostrocaudal position was observed on the increase in signal intensity at week 12 compared to the previous

uninjected imaging session (p = 0.998), and no difference was observed between groups (p = 0.342).

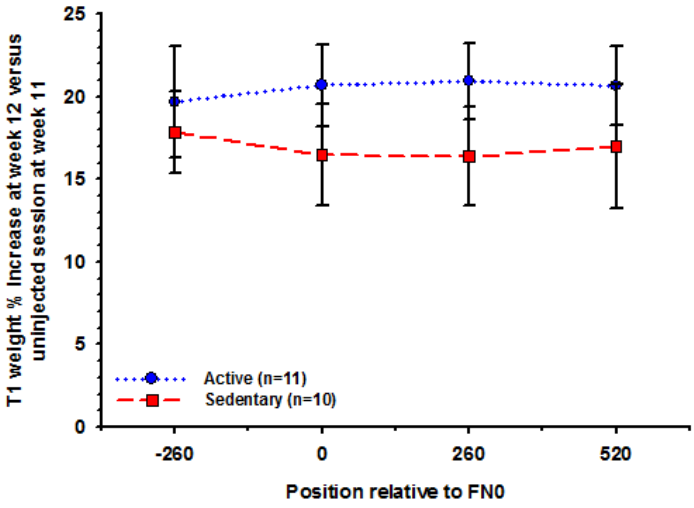


**Figure 16. T1 weighted rostro-caudal analysis of RVLM signal intensity after 12 weeks of sedentary versus physically active conditions.** No differences were observed between groups and there was no significant effect of rostrocaudal position on the percent increase in RVLM intensity at week 12 versus the week 11 values.

## Discussion

The purpose of this study was to use an emerging technique, MEMRI, to longitudinally examine potential differences in *in vivo* neuronal activity within the RVLM, the primary regulator of SNA, of sedentary versus physically active rats. In MEMRI, the paramagnetic ion $Mn^{2+}$ is taken up primarily via L-type calcium channels during action potentials, and is used as an activity-dependent contrast agent to identify regions within the brain that have higher neuronal activity (Ulyanova, et al., 2017; Wang, et al., 2015; Nasu, et al., 1995). We imaged the RVLM before and after administration of $Mn^{2+}$ via chronic i.p. catheter to establish baseline and injected signal intensities before subjecting rats to sedentary or physically active conditions. Rats were imaged again, before and after a second administration of $Mn^{2+}$, to identify potential differences in resting neuronal activity which may have developed due to differences in levels of physical activity. This study was designed based on other studies which have reported differences in voxel enhancement between experimental and control groups ranging

from up to 40% when measured by T1 Weighted analysis, and up to ½ second shift in T1 when measured by T1 map (Holt, et al., 2010; Weng, et al., 2007; Ulyanova, et al., 2017; Kuo, et al., 2007; Zubcevic, et al., 2014; Kim, et al., 2011; Brozoski, et al., 2007). Under those conditions, we calculated that to achieve statistical power of greater than 0.8 to show differences in RVLM activity due to sedentary versus physically active conditions, a need only 8 animals per group when using T1 weighted analysis, or 4 animals per group when using T1 map analysis. In these studies, we compared 11 physically active versus 10 sedentary rats for T1 weighted studies, and 11 physically active versus 9 sedentary animals for T1 map studies.

In this study we have performed both T1 weighted and T1 map imaging of the RVLM in order to examine differences in neuronal activity between sedentary and physically active rats. T1 map imaging was performed on 400μm caudal and rostral sections of the RVLM at 105x105 μm mediolateral and dorsoventral resolution. Sections were separated by the caudal pole of the facial nucleus, with 1/T1 values being correlated with manganese concentrations within the tissues imaged (Chuang, et al., 2009). While T1 map reported valuable information about $Mn^{2+}$ concentrations in the RVLM, imaging required approximately 30 minutes and data obtained via this method is restricted to only areas located in the 2 coronal sections imaged. In contrast, our method of T1 weighted imaging also required approximately 30 minutes, but produced images of the entire brain, from olfactory bulbs to spinomedullary junction, in 260μm coronal slices at 130x130 μm mediolateral and dorsoventral resolution. This additional T1 weighted data can then be analyzed to test hypotheses about other regions of the brain that may also be affected by sedentary versus physically active conditions. Indeed, we are currently examining other regions of the brain involved in

control of SNA.

We have reported the results of The T1 weighted portion of this study as unprocessed voxel intensity within the RVLM, as well as a percent change in T1 weighted signal intensity compared to intensities obtained during pre-injected baseline imaging sessions. Van de Moortele et al. have demonstrated that expressing unprocessed voxel intensity as a ratio of MPRAGE divided by PDGE images produces images which are largely free of errors that may be produced by some technical issues such as inhomogeneity in the magnetic field and the distance between the imaging coil and the tissue being evaluated (Van de Moortele, et al., 2009). However, this correction cannot account for potential differences in signal intensity between individuals. For this reason, we have also expressed signal intensity as a percent change in T1 weighted post-injection signal intensity compared to intensities obtained during pre-injected baseline imaging sessions.

While some groups have used normalization to baseline values to measure neuronal activity, other groups studying different regions of the brain have used a variety of other techniques to normalize MEMRI data, including normalization to muscle, nearby areas of brain tissue, and saline (Matsuda, et al., 2010; Eschenko, et al., 2012; Kuo, et al., 2007; Eschenko, et al., 2010a; Pautler, et al., 1998). However, our group has previously demonstrated that normalizing RVLM intensity to baseline imaging sessions gives a pattern of manganese efflux over time that more closely resembles T1 map imaging, which reflects tissue manganese concentration and does not require normalization, than is obtained by normalizing to different muscle groups or cerebrospinal fluid (Huereca, et al., 2017).

In this study, we report a significant main effect of manganese administration via

chronic i.p. catheter, resulting in increases in RVLM intensity both at week 0 and at week 12, before and after, respectively, exposure to physically active versus sedentary conditions. We also saw a significant main effect of time when measured by unprocessed T1 weighted voxel intensity, as well as an interaction between time and manganese. These data alone would suggest that more manganese is taken up by the RVLM of older animals than is observed in younger animals. This explanation is plausible, as other studies have shown that SNA increases with age in some rat models, and calcium uptake in hippocampal neurons increases with age, as indicated by MEMRI (Bissig and Berkowitz, 2014; Judy and Farrell, 1979). Indeed, both unprocessed T1 weighted and T1 map imaging revealed a significantly greater uptake of $Mn^{2+}$ following administration at week 12 than is observed at week 0, and T1 weighted imaging expressed as a percent increase above baseline values showed an increase that was nearly significant by our criteria at $p=0.06$. However, this interpretation must be viewed with care for two reasons. One reason is that T1 weighted imaging showed a slight but significant increase in RVLM intensity at the week 11 non-injected imaging session compared to the week -1 non-injected session. Our previous study demonstrated that following administration of 66 mg/kg $Mn^{2+}$, signal intensities return to levels not significantly different from baseline after 2-3 weeks (Huereca, et al., 2017). This suggests that the week 11 signal may have been increased for reasons other than $Mn^{2+}$, or due to accumulation of $Mn^{2+}$ from dietary sources or sources other than the previous i.p. administration. However, this potential additional source of $Mn^{2+}$ is unable to account for a second reason to carefully interpret the age-related increase in T1 weighted signal intensity; that is, no significant increase from week -1 to week 11 was detected by T1 map imaging. However, as T1 map and

T1 weighted imaging were performed measuring slightly different amounts of tissue, it is possible that both sets of results are valid for their respective tissue examined and the results of each technique should be judged separately.

We hypothesized there would be an increased signal intensity in the RVLM of rats following 12 weeks of exposure to sedentary conditions compared to rats exposed to 12 weeks of physically active (spontaneous wheel running) conditions. This hypothesis was based on previous studies from our group which demonstrated an increased resting level of SSNA in anesthetized sedentary versus physically active rats, potentially arising from increased efferent signals originating in presympathetic regions such as the RVLM (Subramanian and Mueller, 2016; Mischel and Mueller, 2011). Supporting the hypothesis that the RVLM may be the source of increased sympathetic outflow in sedentary animals, these same studies also reported enhanced SSNA following microinjection of the excitatory amino acid, glutamate, directly into the RVLM in sedentary animals compared to physically active controls, as well as a greater effect on SSNA when injected into rostral areas of the RVLM (Subramanian and Mueller, 2016; Mischel and Mueller, 2011). Other studies have also reported potential differences in RVLM activity due to differences in levels of physical activity. For example Ichiyama et al. reported that following a single bout of exercise, sedentary rats had significantly more RVLM neurons with c-Fos immunoreactivity than were observed in exercise trained rats, suggesting a greater number of neurons were activated (Ichiyama, et al., 2002). Similarly, Greenwood et al. showed significantly enhanced c-Fos expression in the RVLM of sedentary versus exercise trained rats following a sympathoexcitatory stimulus in the form of electrical shock of the tail (Greenwood, et al., 2003). Taken together, these studies suggest that neurons in the RVLM of sedentary

rats may be more active under resting conditions and, and more responsive to sympathoexcitatory stimuli, than those in physically active rats, presumably due to increased levels of glutamate. However it is also possible that the increase in resting SSNA, and the enhanced increase in SSNA following microinjection of glutamate, is due to enhanced sensitivity as a result of a decrease in glutamatergic release in the RVLM, i.e., compensating for decreased glutamatergic neurotransmission either by increasing sensitivity to glutamate or by decreasing sensitivity to inhibitory stimuli. Our group has recently begun examining this possibility through the use of microinjections of antagonists of $GABA_A$ and glutamate receptors to find differences in tonic levels of neurotransmission in the RVLM of anesthetized sedentary and physically active rats.

Despite the supporting evidence in previous studies that led to these experiments, the results reported in this study do not support the hypothesis that neuronal activity within the RVLM changes as a result of sedentary versus physically active conditions. After 12 weeks of sedentary versus physically active conditions, we did not observe different differences in neuronal activity between groups using either T1 weighted or T1 map MEMRI. One reason for the inability to show differences in neuronal activity between groups may be due to the fact that while MEMRI is known to detect differences in total neuronal activity (Massaad and Pautler, 2011), it may not have the temporal resolution to detect differences in neuronal activity if the differences are in the form of changes in patterns of discharge that do not affect the total level of activity during the period of manganese uptake. For example, it has been reported that decreases in human vascular conductance, mediated by muscle sympathetic nerve activity, are encoded for by both SNA burst frequency as well as burst amplitude (Fairfax, et al., 2013). In Fairfax et al. (2013), evidence is offered to suggest that for an

equal amount of total SNA, bursts of consistent amplitude may have a greater effect on vasomotor tone than is caused by more frequent bursts of lower amplitude. If a similar phenomenon occurred within the RVLM, it is possible that the previously reported differences in SSNA between sedentary and physically active rats could be the result of differences in patterns of neuronal activity, despite having the same total level of neuronal activity, and the same amount of signal enhancement when measured by MEMRI. Indeed, it has been reported that while inhibition of the RVLM in rabbits via microinjection of two different compounds produced an identical reduction in total renal sympathetic nerve activity, the reduction in total SNA was either due to decreases in both burst frequency and amplitude, or due to decreases in amplitude alone, depending on the compound used (Head and Burke, 2000).

Another potential reason for the lack of an observable difference in neuronal activity between sedentary and physically active rats is that although the RVLM is considered the primary regulator of SNA, it is not the only regulator of SNA. Studies that have used pseudorabies virus injected into sympathetic ganglia to retrograde label spinally projecting regions of the brain have indicated that in addition to the RVLM, the ventromedial medulla, the raphe nuclei, the paraventricular nucleus of the hypothalamus, and the A5 region are all involved in control of SNA (Strack, et al., 1989). It is possible that the chronically elevated SNA observed in conditions related to CVD may be a result of increased neuronal activity in regions other than the RVLM, or may be due to multiple regions exhibiting small increases in neuronal activity that could be below the level which is detectable by MEMRI. These possibilities are already being investigated by our group, examining other regions involved in control of SNA in addition to the RVLM.

A third potential reason for the lack of observed difference in neuronal activity is the possibility that resting neuronal activity of RVLM neurons may not have been different between the groups of rats used in this study. In Chapter 2 of this dissertation, unit activity of individual RVLM neurons and SSNA were assessed in anesthetized sedentary and physically active rats. However, no differences were found in resting SSNA between groups, as was reported in the previous studies which examined SSNA in rats which were slightly younger (10-12 weeks of sedentary versus physically active conditions) (Mischel and Mueller, 2011;Subramanian and Mueller, 2016). The possibility that resting activity of neurons in the RVLM may not be different between groups is indirectly supported by another recent study from our group that also did not find significant differences in resting SSNA in rats exposed to 12–15 weeks of sedentary versus physically active rats (Dombrowski and Mueller, 2017). It is possible that there was an effect of age or some factor associated with age (e.g., a decrease in running wheel activity) which was able to reduce or eliminate the hypothesized differences RVLM activity between sedentary and physically active rats.

**Technical limitations**

MEMRI indicates changes in activity via uptake of the contrast agent, manganese, into neurons via voltage-gated calcium channels. In its divalent cationic form, manganese can have toxic effects at high concentrations (Eschenko, et al., 2010b; Wendland, 2004; Bock, et al., 2008). In this study, the manganese used was not administered in concentrations shown to produce toxic effects, 66 mg/kg (Eschenko, et al., 2010b; Wendland, 2004; Bock, et al., 2008). Some studies using slightly larger doses have reported that rats exhibited mild symptoms of toxicity (e.g., weight loss and lethargy at 80 mg/kg doses) following manganese administration (Eschenko, et al.,

2010b; Bock, et al., 2008). While lethargy was not measured in this study, rats weighed significantly less at week 12, following administration of manganese, than they did at the week 11 imaging sessions, suggesting that imaging and administration of $Mn^{2+}$ may have induced some physiological stress. While the combined effects of imaging and manganese administration resulted in significant weight loss between week 11 and week 12, the animals did not lose an amount of body weight great enough to meet exclusionary criteria for removal from the study (20% or more). On average, weight loss from week 11 to week 12 was 8 ± 1% in sedentary rats compared to 5 ± 1% in physically active rats, and the amount of weight lost was not significantly different between groups (two-tailed t-test, $p = 0.09$), suggesting that differences in levels of physical activity did not alter responses to manganese administration. One possible explanation for the loss of weight across groups from week 11 to week 12 is dehydration due to the stress of manganese administration and repeated imaging. If administration of manganese introduces physiological alterations, such as pain or dehydration, there may be an increase in neuronal activity among regions of the brain involved in control of SNA, such as the RVLM or the paraventricular nucleus of the hypothalamus (PVH) (Stocker, et al., 2004; Toney, et al., 2003). It is possible that an increase in neuronal activity occurred within the PVH, an area that is known to project to, and alter neuronal activity within the RVLM (Stocker, et al., 2004; Toney, et al., 2003). This possibility is currently being investigated by our laboratory using the library of T1 weighted images collected during this study. Manganese-induced increases in neuronal activity could result in a misinterpretation of the true effect caused by sedentary versus physically active conditions. Ultimately, the potential effects of manganese administration should be considered in the design of experiments so as not

to confound interpretation of the results.

An important technical limitation of MEMRI to consider is that of specificity. While MEMRI is able to demonstrate changes in the general level of neuronal activity, it is unable to indicate which types of cells are taking up and accumulating $Mn^{2+}$ (Kikuta, et al., 2015). Thus, interpretation of neuronal activity could be confounded by heterogeneity of neurons. Though the RVLM is known for its population of barosensitive presympathetic neurons (Guyenet, 2006; Schreihofer and Guyenet, 2002), the region has also been shown to contain respiratory-related glycinergic inhibitory neurons (Schreihofer, et al., 1999). Therefore it is possible that if presympathetic neurons in sedentary rats were more active than those in physically active rats, this difference could be masked if the activity of glycinergic neurons was greater in physically active animals.

Another factor to consider in using MEMRI is that of resolution. In this study, four 260 μm thick virtual slices of the RVLM were used to assess neuronal activity by T1 weighted imaging. While the rostrocaudal range of tissue in this study is similar to the aforementioned structural study on which these experiments were based (Mischel, et al., 2014), the previous study examined the RVLM in six 150 μm tissue sections. It is therefore possible that the resolution at which the images in this study were obtained could be insufficient to demonstrate differences in neuronal activity if there were multiple small regions in the RVLM that responded differently to the experimental procedures. Indeed, recent evidence supports the idea that subregional neuroplasticity occurs in the RVLM as a result of sedentary versus physically active conditions, and that different regions of the RVLM may be differentially control separate sympathetic nerves (Subramanian and Mueller, 2016). Similarly, the region traditionally defined as the

RVLM in coronal sections is larger than the area where the bulk of presympathetic neurons are found (Schreihofer and Guyenet, 1997; Llewellyn-Smith and Mueller, 2013). For these reasons, studies using MEMRI should carefully consider the resolution at which images are obtained and the potential for subregional variability in image intensity, and consider separately examining subregions within a region of interest.

**Perspectives**

Similar to the findings in Chapter 2 of this dissertation, which examined RVLM neurons by extracellular recording, we did not find significant differences in neuronal activity within the RVLM of sedentary versus physically active groups using MEMRI. This result was consistent between T1 map and T1 weighted imaging, and with regard to position along the rostrocaudal axis of the RVLM. While these results are indeed self-supporting, the limitations inherent to MEMRI should be weighed into interpretations. It is known that administration of $Mn^{2+}$ for MEMRI can introduce the potential for physiological stress (Eschenko, et al., 2010b; Wendland, 2004), which may confound interpretation of data for areas of the brain involved in responses to stress. Future studies using MEMRI to examine the effect of risk factors for CVD might do well to use $Mn^{2+}$ at lower doses than used in this study, provided such doses still induce significant increases in signal intensity within the RVLM (Huereca, et al., 2017), or administer $Mn^{2+}$ more slowly (e.g., via osmotic minipump) to reduce the stress caused by subcutaneous, i.p., or i.v. administration (Bock, et al., 2008). Future studies would also do well to consider the resolution at which MEMRI images the RVLM. Some MRI systems may be unable to detect regional differences in neuronal activity due to subregional organization in small animals such as mice and rats (Subramanian and

Mueller, 2016; Mueller, et al., 2011). Larger animals might be better models for MEMRI studies, if the purpose of those studies is to examine differential control of sympathetic nerves due to subregional organization of the RVLM.

# CHAPTER 4 - CONCLUSIONS AND PERSPECTIVES

The purpose of these studies was to examine the role of the RVLM in generating the different levels of SSNA previously reported between sedentary and physically active rats (Mischel and Mueller, 2011; Subramanian and Mueller, 2016). The hypotheses were; 1) RVLM neurons in sedentary rats would exhibit increased resting activity and a larger response to sympathoexcitatory stimuli compared to what would be observed in physically active rats, consistent with increased sympathetic outflow; 2) these neurons would also exhibit increased dendritic arborization in physically active animals, similar to that which was previously reported; and 3) assessment of general neuronal activity in the RVLM using MEMRI would show enhanced RVLM activity in sedentary versus physically active rats. Chapter 2 examined the first hypothesis by obtaining extracellular recordings of neurons in the RVLM of anesthetized rats and assessing baroreflex sensitivity via intravenous infusion of SNP and PE. The second hypothesis was also examined in Chapter 2 by juxtacellularly labeling neurons which had been assessed for barosensitivity. Finally, the third hypothesis was examined in Chapter 3 by examining neuronal activity in the RVLM of awake, freely behaving sedentary and physically active rats using MEMRI.

The main findings of these studies were; 1) barosensitive RVLM neurons did not show differences between sedentary and physically active rats in terms of resting frequency, maximum or minimum frequency, or slope of baroreflex curves; 2) though a small sample size (n=4 neurons from sedentary rats, n=7 neurons from physically active rats) prevents us from making a firm conclusion from this experiment, barosensitive RVLM neurons did not show differences between sedentary and physically active rats in terms of dendritic length or arborization; 3) resting neuronal activity within the RVLM

was not different between awake sedentary and physically active rats, as examined for the first time in awake rats using MEMRI.

The general hypothesis behind these experiments was that activity of RVLM neurons would be greater in sedentary versus physically active animals. This hypothesis was based on previous studies from our group which showed enhanced increases in SSNA in sedentary versus physically active rats following baroreceptor unloading via i.v. infusion of SNP or microinjection of the excitatory amino acid, glutamate, directly into the RVLM (Mischel and Mueller, 2011; Subramanian and Mueller, 2016), and that the RVLM bulbospinal C1 neurons exhibited enhanced dendritic branching and length in sedentary rats compared to physically active counterparts (Mischel, et al., 2014). The significance of those studies was that they provided strong evidene of neuroplastic changes in the RVLM that may explain increases in SNA that are associated with a sedentary lifestyle, a major risk factor for CVD in humans (Malpas, 2010; Thom, et al., 2006; Mueller, 2007). However, extracellular recordings of individual RVLM neurons in anesthetized animals, and assessment of general neuronal activity in the RVLM of awake animals via MEMRI were unable to demonstrate differences in neuronal activity between sedentary and physically active rats. Similarly, these experiments were unable to demonstrate differences in SSNA between groups of animals, an effect which was observed in some studies previously published by our group (Mischel and Mueller, 2011; Subramanian and Mueller, 2016). It is important to note that this study used slightly different models than the previous studies, with the animals in this study being slightly older, and so the results might not be directly comparable. A study recently published by our group (Dombrowski and Mueller, 2017) using animals approximately the same age as those in

this study did not observe differences in resting SSNA between groups observed in the previously mentioned studies. These data, along with other unpublished observations from our group suggest that age, or some factor associated with age (e.g., a decrease in running wheel activity) may be able to reduce the differences in SSNA observed between younger sedentary and physically active rats.

The original question remains unanswered by the experiments presented in this dissertation; were the differences in SSNA seen between rats after 10-12 weeks of sedentary versus physically active conditions a result of changes in the RVLM? While it is accepted that the RVLM is the primary regulator of SNA (Guyenet, 2006; Ross, et al., 1984b; Schreihofer and Guyenet, 2002), it is possible that other regions involved in autonomic control may contribute to the observed differences in SSNA. For example, neurons of the PVH are known to have excitatory glutamatergic projections to the RVLM (Stocker, et al., 2006), and have also been shown to have collateral axonal projections to the spinal cord and a correlation with SNA (Chen and Toney, 2010). It is also interesting to note that nearly complete inhibition of SSNA can occur despite only partial inhibition of the RVLM (Schreihofer and Guyenet, 2000a), suggesting that the activity of RVLM neurons alone may not be sufficient to maintain SSNA in some circumstances.

Ideally, animal models measuring neuronal activity in regions of the brain involved in autonomic control would be conducted *in vivo*, in a way that can examine multiple regions in the same animal, longitudinally. While MEMRI is one attempt to do this, the model used in these experiments is not directly translational to human studies due to the toxicity of $Mn^{2+}$ in humans (Guilarte, 2013; Dobson, et al., 2004). However, advances in the techniques used may make MEMRI in humans possible in the future. One manganese-containing MRI contrast agent was previously approved for use in

human liver imaging (Federle, et al., 2000a) and did not show clinically significant short-term risks (Federle, et al., 2000b). Theoretically, it is possible that in time, emerging technologies will allow us to test if risk factors for CVD the activity of neurons that affect SNA in animal models, and see if these changes translate to human models as well.

# APPENDIX

## IACUC Protocol Approval Letter

WAYNE STATE UNIVERSITY

INSTITUTIONAL ANIMAL
CARE AND USE COMMITTEE
87 E. Canfield, Second Floor
Detroit, MI 48201-2011
Telephone: (313) 577-1629
Fax Number: (313) 577-1941

**ANIMAL WELFARE ASSURANCE # A3310-01**

**PROTOCOL # A 11-07-14**

**Protocol Effective Period: December 22, 2014 – November 30, 2017**

**Year 2 Annual Review Date: December 1, 2015**
**Year 3 Annual Review Date: December 1, 2016**

**TO:** Dr. Patrick Mueller
Physiology
School of Medicine
5263 Scott Hall

**FROM:** Lisa Anne Polin, Ph.D.
Chairperson
Institutional Animal Care and Use Committee

**SUBJECT:** Approval of Protocol # A 11-07-14

"Inactivity and Enhanced Sympathoexcitation: Role of Neuroplasticity in the RVLM (rostral ventrolateral medulla)"

**DATE:** December 01, 2016

The Annual Review of your animal research protocol and any applicable grant applications has been conducted and approved by the Wayne State University Institutional Animal Care and Use Committee (IACUC). The species and number of animals approved for the duration of this protocol are listed below.

| Species | Strain | Qty. | Cat. |
|---|---|---|---|
| RATS | NIH, R01,Sprague Dawley, Male, Adults | 176 | C |
| RATS | NIH, R01, Sprague Dawley, Male, Adults | 694 | D |
| RATS | NIH, R01,Sprague Dawley, Male, Adults | 36 | D |

| Species Amendments | Strain | Qty. | Cat. |
|---|---|---|---|
| MICE | C57BL/6 WT, MALE, | | |
| 15-20 weeks old | 10 | | D |
| MICE | C57BL/6 TPH2 KO, MALE, | | |
| 15-20 weeks old | 10 | | D |

**Be advised** that any change in the procedures used, a change in species, or additional numbers of animals requires prior approval by the IACUC. Any animal work on this research protocol beyond the expiration date will require the submission of a new IACUC protocol form and full committee review.

The Guide for the Care and Use of Laboratory Animals is the primary reference used for standards of animal care at Wayne State University. The University has submitted an appropriate assurance statement to the Office of Laboratory Animal Welfare (OLAW) of the National Institutes of Health. The animal care program at Wayne State University is accredited by the Association for Assessment and Accreditation of Laboratory Animal Care International (AAALAC).

## REFERENCES


1. Agarwal SK and Calaresu FR (1991) Monosynaptic connection from caudal to rostral ventrolateral medulla in the baroreceptor reflex pathway. *Brain Res: 555*70-74.
2. Almado CE, Leao RM and Machado BH (2014) Intrinsic properties of rostral ventrolateral medulla presympathetic and bulbospinal respiratory neurons of juvenile rats are not affected by chronic intermittent hypoxia. *Exp Physiol* 99:937-950.
3. Aoki I, Wu YJ, Silva AC, Lynch RM and Koretsky AP (2004) In vivo detection of neuroarchitecture in the rodent brain using manganese-enhanced MRI. *Neuroimage* 22:1046-1059.
4. Barnes MJ and McDougal DH (2014) Leptin into the rostral ventral lateral medulla (RVLM) augments renal sympathetic nerve activity and blood pressure. *Front Neurosci* 8:232.
5. Beatty JA, Kramer JM, Plowey ED and Waldrop TG (2005) Physical exercise decreases neuronal activity in the posterior hypothalamic area of spontaneously hypertensive rats. *J Appl Physiol* 98:572-578.
6. Bissig D and Berkowitz BA (2011) Same-session functional assessment of rat retina and brain with manganese-enhanced MRI. *Neuroimage* 58:749-760.
7. Bissig D and Berkowitz BA (2014) Testing the calcium hypothesis of aging in the rat hippocampus in vivo using manganese-enhanced MRI. *Neurobiol Aging* 35:1453-1458.
8. Bock NA, Paiva FF and Silva AC (2008) Fractionated manganese-enhanced MRI. *NMR Biomed* 21:473-478.

9. Booth FW, Laye MJ, Lees SJ, Rector RS and Thyfault JP (2007) Reduced physical activity and risk of chronic disease: the biology behind the consequences. *Eur J Appl Physiol*.

10. Brown DL and Guyenet PG (1984) Cardiovascular neurons of brain stem with projections to spinal cord. *Am J Physiol* 247:R1009-R1016.

11. Brown DL and Guyenet PG (1985) Electrophysiological study of cardiovascular neurons in the rostral ventrolateral medulla in rats. *Circ Res* 56:359-369.

12. Brozoski TJ, Ciobanu L and Bauer CA (2007) Central neural activity in rats with tinnitus evaluated with manganese-enhanced magnetic resonance imaging (MEMRI). *Hear Res* 228:168-179.

13. Burke PG, Neale J, Korim WS, McMullan S and Goodchild AK (2011) Patterning of somatosympathetic reflexes reveals nonuniform organization of presympathetic drive from C1 and non-C1 RVLM neurons. *Am J Physiol Regul Integr Comp Physiol* 301:R1112-R1122.

14. Cassell MD and Gray TS (1989) The amygdala directly innervates adrenergic (C1) neurons in the ventrolateral medulla in the rat. *Neurosci Lett* 97:163-168.

15. Chan RKW and Sawchenko PE (1994) Spatially and temporally differentiated patterns of *c-fos* expression in brainstem catecholaminergic cell groups induced by cardiovascular challenges in the rat. *J Comp Neurol* 348:433-460.

16. Charkoudian N (2010) Heterogeneity in human cardiovascular function contributes to a deeper understanding of integrative mechanisms. *J Appl Physiol* 108:473-474.

17. Charkoudian N and Rabbitts JA (2009) Sympathetic neural mechanisms in human cardiovascular health and disease. *Mayo Clin Proc* 84:822-830.

18. Chen QH and Toney GM (2003) Identification and characterization of two functionally distinct groups spinal cord projecting paraventricular nucleus neurons with sympathetic related activity. *Neuroscience* 118:797-807.

19. Chen QH and Toney GM (2010) In vivo discharge properties of hypothalamic paraventricular nucleus neurons with axonal projections to the rostral ventrolateral medulla. *J Neurophysiol* 103:4-15.

20. Chuang KH and Koretsky AP (2009) Accounting for nonspecific enhancement in neuronal tract tracing using manganese enhanced magnetic resonance imaging. *Magn Reson Imaging* 27:594-600.

21. Chuang KH, Koretsky AP and Sotak CH (2009) Temporal changes in the T1 and T2 relaxation rates (DeltaR1 and DeltaR2) in the rat brain are consistent with the tissue-clearance rates of elemental manganese. *Magn Reson Med* 61:1528-1532.

22. Cravo SL and Morrison SF (1993) The caudal ventrolateral medulla is a source of tonic sympathoinhibition. *Brain Res* 62:133-136.

23. Dampney RAL (1994) The subretrofacial vasomotor nucleus: anatomical, chemical and pharmacological properties and role in cardiovascular regulation. *Prog Neurobiol* 42:197-227.

24. Dampney RAL, Blessing WW and Tan E (1988) Origin of tonic GABAergic inputs to vasopressor neurons in the subretrofacial nucleus of the rabbit. *J Auton Nerv Syst* 24:227-239.

25. Dampney RAL, Czachurski J, Dembowsky K, Goodchild AK and Seller H (1987) Afferent connections and spinal projections of the pressor region in the rostral ventrolateral medulla of the cat. *J Auton Nerv Syst* 20:73-86.

26. Dampney RAL, Fontes MAP, Hirooka Y, Horiuchi J, Potts PD and Tagawa T (2002) Role of angiotensin II receptors in the regulation of vasomotor neurons in the ventrolateral medulla. *Clin Exp Pharmacol Physiol* 29:467-472.

27. Dean C, Seagard JL, Hopp FA and Kampine JP (1992) Differential control of sympathetic activity to kidney and skeletal muscle by ventral medullary neurons. *J Auton Nerv Syst* 37:1-10.

28. Delaney EP, Greaney JL, Edwards DG, Rose WC, Fadel PJ and Farquhar WB (2010) Exaggerated sympathetic and pressor responses to handgrip exercise in older hypertensive humans: role of the muscle metaboreflex. *Am J Physiol Heart Circ Physiol* 299:H1318-H1327.

29. Delorme EJ, Macpherson AI, Mukherjee SR and Rowlands S (1951) Measurement of the visceral blood volume in dogssssss. *Q J Exp Physiol Cogn Med Sci* 36:219-231.

30. DiCarlo SE and Bishop VS (1988) Exercise training attenuates baroreflex regulation of nerve activity in rabbits. *Am J Physiol* 255:H974-H979.

31. Dobson AW, Erikson KM and Aschner M (2004) Manganese neurotoxicity. *Ann N Y Acad Sci* 1012:115-128.

32. Dombrowski MD and Mueller PJ (2017) Sedentary conditions and enhanced responses to GABA in the RVLM: Role of the contralateral RVLM. *Am J Physiol Regul Integr Comp Physiol*.

33. Dorward PK, Riedel W, Burke SL, Gipps G and Korner PI (1985) The renal sympathetic baroreflex in the rabbit - Arterial and cardiac baroreceptor influences, resetting, and effect of anesthesia. *Circ Res* 57:618-633.

34. Eschenko O, Canals S, Simanova I, Beyerlein M, Murayama Y and Logothetis

NK (2010a) Mapping of functional brain activity in freely behaving rats during voluntary running using manganese-enhanced MRI: implication for longitudinal studies. *Neuroimage* 49:2544-2555.

35. Eschenko O, Canals S, Simanova I and Logothetis NK (2010b) Behavioral, electrophysiological and histopathological consequences of systemic manganese administration in MEMRI. *Magn Reson Imaging* 28:1165-1174.

36. Eschenko O, Evrard HC, Neves RM, Beyerlein M, Murayama Y and Logothetis NK (2012) Tracing of noradrenergic projections using manganese-enhanced MRI. *Neuroimage* 59:3252-3265.

37. Fairfax ST, Padilla J, Vianna LC, Davis MJ and Fadel PJ (2013) Spontaneous bursts of muscle sympathetic nerve activity decrease leg vascular conductance in resting humans. *Am J Physiol Heart Circ Physiol* 304:H759-H766.

38. Federle M, Chezmar J, Rubin DL, Weinreb J, Freeny P, Schmiedl UP, Brown JJ, Borrello JA, Lee JK, Semelka RC, Mattrey R, Dachman AH, Saini S, Harms SE, Mitchell DG, Anderson MW, Halford HH, III, Bennett WF, Young SW, Rifkin M, Gay SB, Ballerini R, Sherwin PF and Robison RO (2000a) Efficacy and safety of mangafodipir trisodium (MnDPDP) injection for hepatic MRI in adults: results of the U.S. Multicenter phase III clinical trials. Efficacy of early imaging. *J Magn Reson Imaging* 12:689-701.

39. Federle MP, Chezmar JL, Rubin DL, Weinreb JC, Freeny PC, Semelka RC, Brown JJ, Borello JA, Lee JK, Mattrey R, Dachman AH, Saini S, Harmon B, Fenstermacher M, Pelsang RE, Harms SE, Mitchell DG, Halford HH, Anderson MW, Johnson CD, Francis IR, Bova JG, Kenney PJ, Klippenstein DL, Foster GS and Turner DA (2000b) Safety and efficacy of mangafodipir trisodium (MnDPDP)

injection for hepatic MRI in adults: results of the U.S. multicenter phase III clinical trials (safety). *J Magn Reson Imaging* 12:186-197.

40. Fisher JP, Young CN and Fadel PJ (2009) Central sympathetic overactivity: maladies and mechanisms. *Auton Neurosci* 148:5-15.

41. Foley CM, Mueller PJ, Hasser EM and Heesch CM (2005) Hindlimb unloading and female gender attenuate baroreflex mediated sympathoexcitation. *Am J Physiol Regul Integr Comp Physiol* 289:R1440-R1447.

42. Geraldes CF, Sherry AD, Brown RD, III and Koenig SH (1986) Magnetic field dependence of solvent proton relaxation rates induced by Gd3+ and Mn2+ complexes of various polyaza macrocyclic ligands: implications for NMR imaging. *Magn Reson Med* 3:242-250.

43. Gonzalez ER, Krieger AJ and Sapru HN (1983) Central resetting of baroreflex in the spontaneously hypertensive rat. *Hypertension* 5:346-352.

44. Grassi G, Seravalle G, Calhoun DA and Mancia G (1994) Physical training and baroreceptor control of sympathetic nerve activity in humans. *Hypertension* 23:294-301.

45. Greenberg DM, Copp DH and Cuthbertson EM (1943) Studies in mineral metabolism with the aid of artificial radioactive isotopes. VII. The distribution and excretion, particularly by way of the bile, of iron, cobalt, and manganese. *J Biol Chem* 147:749-756.

46. Greenwood BN, Kennedy S, Smith TP, Campeau S, Day HEW and Fleshner M (2003) Voluntary freewheel running selectively modulates catecholamine content in peripheral tissue and c-fos expression in the central sympathetic circuit following exposure to uncontrollable stress in rats. *Neuroscience* 120:269-281.

47. Guilarte TR (2013) Manganese neurotoxicity: new perspectives from behavioral, neuroimaging, and neuropathological studies in humans and non-human primates. *Front Aging Neurosci* 5:23.

48. Guild SJ, Barrett CJ, McBryde FD, Van Vliet BN, Head GA, Burke SL and Malpas SC (2010) Quantifying sympathetic nerve activity: problems, pitfalls and the need for standardization. *Exp Physiol* 95:41-50.

49. Guyenet PG (2006) The sympathetic control of blood pressure. *Nat Rev Neurosci* 7:335-346.

50. Guyenet PG, Schreihofer AM and Stornetta RL (2001) Regulation of sympathetic tone and arterial pressure by the rostral ventrolateral medulla after depletion of C1 cells in rats. *Ann N Y Acad Sci* 940:259-269.

51. Guyenet PG, Stornetta RL, Bochorishvili G, Depuy SD, Burke PG and Abbott SB (2013) C1 neurons: the body's EMTs. *Am J Physiol Regul Integr Comp Physiol* 305:R187-R204.

52. Hart EC, Joyner MJ, Wallin BG and Charkoudian N (2012) Sex, ageing and resting blood pressure: gaining insights from the integrated balance of neural and haemodynamic factors. *J Physiol* 590:2069-2079.

53. Haselton JR and Guyenet PG (1989) Electrophysiological characterization of putative C1 adrenergic neurons in the rat. *Neuroscience* 30:199-214.

54. Hayward LF, Riley AP and Felder RB (2002) $a_2$-Adrenergic receptors in NTS facilitate baroreflex function in adult spontaneously hypertensive rats. *Am J Physiol Heart Circ Physiol* 282:H2336-H2345.

55. Head GA and Burke SL (2000) Comparison of renal sympathetic baroreflex effects of rilmenidine and alpha-methylnoradrenaline in the ventrolateral medulla

of the rabbit. *J Hypertens* 18:1263-1276.

56. Head GA and Burke SL (2001) Renal and cardiac sympathetic baroreflexes in hypertensive rabbits. *Clin Exp Pharmacol Physiol* 28:972-975.

57. Heidenreich PA, Albert NM, Allen LA, Bluemke DA, Butler J, Fonarow GC, Ikonomidis JS, Khavjou O, Konstam MA, Maddox TM, Nichol G, Pham M, Pina IL and Trogdon JG (2013) Forecasting the impact of heart failure in the United States: a policy statement from the American Heart Association. *Circ Heart Fail* 6:606-619.

58. Holt AG, Bissig D, Mirza N, Rajah G and Berkowitz B (2010) Evidence of key tinnitus-related brain regions documented by a unique combination of manganese-enhanced MRI and acoustic startle reflex testing. *PLoS One* 5:e14260.

59. How JM, Wardak SA, Ameer SI, Davey RA and Sartor DM (2014) Blunted sympathoinhibitory responses in obesity-related hypertension are due to aberrant central but not peripheral signalling mechanisms. *J Physiol* 592:1705-1720.

60. Huang C, Yoshimoto M, Miki K and Johns EJ (2006) The contribution of brain angiotensin II to the baroreflex regulation of renal sympathetic nerve activity in conscious normotensive and hypertensive rats. *J Physiol* 574:597-604.

61. Huber DA and Schreihofer AM (2010) Attenuated baroreflex control of sympathetic nerve activity in obese Zucker rats by central mechanisms. *J Physiol* 588:1515-1525.

62. Huber DA and Schreihofer AM (2011) Altered regulation of the rostral ventrolateral medulla in hypertensive obese Zucker rats. *Am J Physiol Heart Circ Physiol* 301:H230-H240.

63. Huereca DJ, Bakoulas KA, Ghoddousi F, Berkowitz BA, Holt AG and Mueller PJ (2017) Development of Manganese - Enhanced Magnetic Resonance Imaging of the Rostral Ventrolateral Medulla of Conscious Rats: Importance of Normalization and Comparison to Other Regions of Interest. *NMR Biomed* ***In Revision.***

64. Humphrey DR and Schmidt EM (1990) Extracellular single-unit recording methods. *Neuromethods* 15:1-64.

65. Ichiyama RM, Gilbert AB, Waldrop TG and Iwamoto GA (2002) Changes in the exercise activation of diencephalic and brainstem cardiorespiratory areas after training. *Brain Res* 947:225-233.

66. Inoue T, Majid T and Pautler RG (2011) Manganese enhanced MRI (MEMRI): neurophysiological applications. *Rev Neurosci* 22:675-694.

67. Ito K, Sato A, Sato Y and Suzuki H (1986) Increases in adrenal catecholamine secretion and adrenal sympathetic nerve unitary activities with aging in rats. *Neurosci Lett* 69:263-268.

68. Ito S, Hiratsuka M, Komatsu K, Tsukamoto K, Kanmatsuse K and Sved AF (2003) Ventrolateral medulla AT1 Receptors support arterial pressure in Dahl salt-sensitive rats. *Hypertension* 41:744-750.

69. Iwashita S, Tanida M, Terui N, Ootsuka Y, Shu M, Kang D and Suzuki M (2002) Direct measurement of renal sympathetic nervous activity in high-fat diet-related hypertensive rats. *Life Sci* 71:537-546.

70. Jansen ASP, Nguyen XV, Karpitskiy V, Mettenleiter TC and Loewy AD (1995) Central command neurons of the sympathetic nervous system: basis of the fight-or-fight response. *Science* 270:644-646.

71. Judy WV and Farrell SK (1979) Arterial baroreceptor reflex control of sympathetic nerve activity in the spontaneously hypertensive rat. *Hypertension* 1:605-614.

72. Jung DJ, Han M, Jin SU, Lee SH, Park I, Cho HJ, Kwon TJ, Lee HJ, Cho JH, Lee KY and Chang Y (2014) Functional mapping of the auditory tract in rodent tinnitus model using manganese-enhanced magnetic resonance imaging. *Neuroimage* 100:642-649.

73. Kajekar R, Chen C-Y, Mutoh T and Bonham AC (2002) $GABA_A$ receptor activation at medullary sympathetic neurons contributes to postexercise hypotension. *Am J Physiol Heart Circ Physiol* 282:H1615-H1624.

74. Kc P, Balan KV, Tjoe SS, Martin RJ, Lamanna JC, Haxhiu MA and Dick TE (2010) Increased vasopressin transmission from the paraventricular nucleus to the rostral medulla augments cardiorespiratory outflow in chronic intermittent hypoxia-conditioned rats. *J Physiol* 588:725-740.

75. Kenney MJ (2010) Animal aging and regulation of sympathetic nerve discharge. *J Appl Physiol (1985 )* 109:951-958.

76. Kikuta S, Nakamura Y, Yamamura Y, Tamura A, Homma N, Yanagawa Y, Tamura H, Kasahara J and Osanai M (2015) Quantitative activation-induced manganese-enhanced MRI reveals severity of Parkinson's disease in mice. *Sci Rep* 5:12800.

77. Kim J, Choi IY, Michaelis ML and Lee P (2011) Quantitative in vivo measurement of early axonal transport deficits in a triple transgenic mouse model of Alzheimer's disease using manganese-enhanced MRI. *Neuroimage* 56:1286-1292.

78. Krieger EM, Da Silva GJJ and Negrao CE (2001) Effects of exercise training on

baroreflex control of the cardiovascular system. *Ann N Y Acad Sci* 940:338-347.

79. Krout KE, Mettenleiter TC, Karpitskiy V, Nguyen XV and Loewy AD (2005) CNS neurons with links to both mood-related cortex and sympathetic nervous system. *Brain Res* 1050:199-202.

80. Kulics JM, Collins HL and DiCarlo SE (1999) Postexercise hypotension is mediated by reductions in sympathetic nerve activity. *Am J Physiol Heart Circ Physiol* 276:H27-H32.

81. Kuo YT, Herlihy AH, So PW and Bell JD (2006) Manganese-enhanced magnetic resonance imaging (MEMRI) without compromise of the blood-brain barrier detects hypothalamic neuronal activity in vivo. *NMR Biomed* 19:1028-1034.

82. Kuo YT, Parkinson JR, Chaudhri OB, Herlihy AH, So PW, Dhillo WS, Small CJ, Bloom SR and Bell JD (2007) The temporal sequence of gut peptide CNS interactions tracked in vivo by magnetic resonance imaging. *J Neurosci* 27:12341-12348.

83. Laterza MC, de Matos LD, Trombetta IC, Braga AM, Roveda F, Alves MJ, Krieger EM, Negrao CE and Rondon MU (2007) Exercise training restores baroreflex sensitivity in never-treated hypertensive patients. *Hypertension* 49:1298-1306.

84. Lee JH, Silva AC, Merkle H and Koretsky AP (2005) Manganese-enhanced magnetic resonance imaging of mouse brain after systemic administration of MnCl2: dose-dependent and temporal evolution of T1 contrast. *Magn Reson Med* 53:640-648.

85. Li Y-W, Gieroba ZJ, McAllen RM and Blessing WW (1991) Neurons in rabbit caudal ventrolateral medulla inhibit bulbospinal barosensitive neurons in rostral

medulla. *Am J Physiol: 261*R44-R51.

86. Lin YJ and Koretsky AP (1997) Manganese ion enhances T1-weighted MRI during brain activation: an approach to direct imaging of brain function. *Magn Reson Med* 38:378-388.

87. Lipski J, Kanjhan R, Kruszewska B and Rong W (1996) Properties of presympathetic neurones in the rostral ventrolateral medulla in the rat: an intracellular study 'in vivo'. *J Physiol* 490:729-744.

88. Lipski J, Kanjhan R, Kruszewska B and Smith M (1995) Barosensitive neurons in the rostral ventrolateral medulla of the in vivo: morphological properties and relationship to C1 adrenergic neurons. *Neuroscience* 69:601-618.

89. Llewellyn-Smith IJ, DiCarlo SE, Collins HL and Keast JR (2005) Enkephalin-immunoreactive interneurons extensively innervate sympathetic preganglionic neurons regulating the pelvic viscera. *J Comp Neurol* 488:278-289.

90. Llewellyn-Smith IJ and Gnanamanickam GJ (2011) Immunoperoxidase detection of neuronal antigens in full-thickness whole mount preparations of hollow organs and thick sections of central nervous tissue. *J Neurosci Methods* 196:1-11.

91. Llewellyn-Smith IJ and Mueller PJ (2013) Immunoreactivity for the NMDA NR1 subunit in bulbospinal catecholamine and serotonin neurons of rat ventral medulla. *Auton Neurosci*.

92. Lovick TA (1987) Differential control of cardiac and vasomotor activity by neurones in nucleus paragigantocellularis lateralis in the cat. *J Physiol* 389:23-35.

93. Lovick TA and Hilton SM (1985) Vasodilator and vasoconstrictor neurones of the ventrolateral medulla in the cat. *Brain Res* 331:353-357.

94. Luo N, Merrill P, Parikh KS, Whellan DJ, Pina IL, Fiuzat M, Kraus WE, Kitzman DW, Keteyian SJ, O'Connor CM and Mentz RJ (2017) Exercise Training in Patients With Chronic Heart Failure and Atrial Fibrillation. *J Am Coll Cardiol* 69:1683-1691.

95. Madden CJ, Ito S, Rinaman L, Wiley RG and Sved AF (1999) Lesions of the C1 catecholaminergic neurons of the ventrolateral medulla in rats using anti-DbH-saporin. *Am J Physiol Regul Integr Comp Physiol* 277:R1063-R1075.

96. Malheiros JM, Paiva FF, Longo BM, Hamani C and Covolan L (2015) Manganese-Enhanced MRI: Biological Applications in Neuroscience. *Front Neurol* 6:161.

97. Malpas SC (2010) Sympathetic nervous system overactivity and its role in the development of cardiovascular disease. *Physiol Rev* 90:513-557.

98. Mandel DA and Schreihofer AM (2006) Central respiratory modulation of barosensitive neurones in rat caudal ventrolateral medulla. *J Physiol* 572:881-896.

99. Massaad CA and Pautler RG (2011) Manganese-enhanced magnetic resonance imaging (MEMRI). *Methods Mol Biol* 711:145-174.

100. Matsuda K, Wang HX, Suo C, McCombe D, Horne MK, Morrison WA and Egan GF (2010) Retrograde axonal tracing using manganese enhanced magnetic resonance imaging. *Neuroimage* 50:366-374.

101. McAllen RM, Habler HJ, Michaelis M, Peters O and Janig W (1994) Monosynaptic excitation of preganglionic vasomotor neurons by subretrofacial neurons of the rostral ventrolateral medulla. *Brain Res* 634:227-234.

102. Mendis S, Armstrong T, Bettcher D, Branca F, Lauer J, Mace C, Poznyak V,

Riley L, Da Costa E Silva V and Stevens G. Global status report on noncommunicable diseases 2014. 2014. World Health Organization, 2015.

103. Mendis S, Puska P and Norrving B. Global atlas on cardiovascular disease prevention and control. 2011.

104. Mendonca-Dias MH, Gaggelli E and Lauterbur PC (1983) Paramagnetic contrast agents in nuclear magnetic resonance medical imaging. *Semin Nucl Med* 13:364-376.

105. Miki K, Yoshimoto M and Tanimizu M (2003) Acute shifts of baroreflex control of renal sympathetic nerve activity induced by treadmill exercise in rats. *J Physiol: 548 1*313-322.

106. Mischel NA, Llewellyn-Smith IJ and Mueller PJ (2014) Physical (in)activity-dependent structural plasticity in bulbospinal catecholaminergic neurons of rat rostral ventrolateral medulla. *J Comp Neurol* 522:499-513.

107. Mischel NA and Mueller PJ (2011) (In)activity-dependent alterations in resting and reflex control of splanchnic sympathetic nerve activity. *J Appl Physiol* 111:1854-1862.

108. Mischel NA, Subramanian M, Dombrowski MD, Llewellyn-Smith IJ and Mueller PJ (2015) (In)activity-Related Neuroplasticity in Brainstem Control of Sympathetic Outflow: Unraveling Underlying Molecular, Cellular and Anatomical Mechanisms. *Am J Physiol Heart Circ Physiol*ajpheart.

109. Moffitt JA, Foley CM, Schadt JC, Laughlin MH and Hasser EM (1998) Attenuated baroreflex control of sympathetic nerve activity after cardiovascular deconditioning in rats. *Am J Physiol Regul Integr Comp Physiol* 274:R1397-R1405.

110. Morgan DA, Anderson EA and Mark AL (1995) Renal sympathetic nerve activity is increased in obese Zucker rats. *Hypertension* 25:834-838.

111. Mueller PJ (2007) Exercise training and sympathetic nervous system activity: evidence for physical activity dependent neural plasticity. *Clin Exp Pharmacol Physiol* 34:377-384.

112. Mueller PJ (2010) Physical (in)activity-dependent alterations at the rostral ventrolateral medulla: influence on sympathetic nervous system regulation. *Am J Physiol Regul Integr Comp Physiol* 298:R1468-R1474.

113. Mueller PJ and Mischel NA (2012) Selective enhancement of glutamate-mediated pressor responses after GABA(A) receptor blockade in the RVLM of sedentary versus spontaneous wheel running rats. *Front Physiol* 3:447.

114. Mueller PJ, Mischel NA and Scislo TJ (2011) Differential activation of adrenal, renal, and lumbar sympathetic nerves following stimulation of the rostral ventrolateral medulla of the rat. *Am J Physiol Regul Integr Comp Physiol* 300:R1230-R1240.

115. Muller-Ribeiro FC, Dampney RA, McMullan S, Fontes MA and Goodchild AK (2014) Disinhibition of the midbrain colliculi unmasks coordinated autonomic, respiratory, and somatomotor responses to auditory and visual stimuli. *Am J Physiol Regul Integr Comp Physiol* 307:R1025-R1035.

116. Muntzel MS, Al-Naimi OA, Barclay A and Ajasin D (2012) Cafeteria diet increases fat mass and chronically elevates lumbar sympathetic nerve activity in rats. *Hypertension* 60:1498-1502.

117. Myers J, Prakash M, Froelicher V, Do D and Atwood J (2002) Exercise capacity and mortality among men referred for exercise testing. *N Engl J Med* 346:793-

801.

118. Narkiewicz K and Somers VK (1997) The sympathetic nervous system and obstructive sleep apnea: implications for hypertension. *J Hypertens* 15:1613-1619.

119. Nasu T, Murase H and Shibata H (1995) Manganese ions penetrate via L-type Ca2+ channels and induce contraction in high-K+ medium in ileal longitudinal muscle of guinea-pig. *Gen Pharmacol* 26:381-386.

120. Nelson AJ, Juraska JM, Musch TI and Iwamoto GA (2005) Neuroplastic adaptations to exercise: neuronal remodeling in cardiorespiratory and locomotor areas. *J Appl Physiol* 99:2312-2322.

121. Nelson AJ, Juraska JM, Ragan BG and Iwamoto GA (2010) Effects of exercise training on dendritic morphology in the cardiorespiratory and locomotor centers of the mature rat brain. *J Appl Physiol (1985 )* 108:1582-1590.

122. Oshima N, McMullan S, Goodchild AK and Pilowsky PM (2006) A monosynaptic connection between baroinhibityed neurons in the RVLM and IML in Sprague-Dawley rats. *Brain Res* 1089:153-161.

123. Owens NC, Sartor DM and Verberne AJM (1999) Medial prefrontal cortex depressor response: role of the solitary tract nucleus in the rat. *Neuroscience* 89:1331-1346.

124. Paton JF, Boscan P, Pickering AE and Nalivaiko E (2005) The yin and yang of cardiac autonomic control: vago-sympathetic interactions revisited. *Brain Res Brain Res Rev* 49:555-565.

125. Pautler RG, Silva AC and Koretsky AP (1998) In vivo neuronal tract tracing using manganese-enhanced magnetic resonance imaging. *Magn Reson Med* 40:740-

748.

126. Paxinos G and Watson C (2007) *The rat brain in stereotaxic coordinates*. Elsevier Inc., Burlington, MA.

127. Pedrino GR, Calderon AS, Andrade MA, Cravo SL and Toney GM (2013) Discharge of RVLM vasomotor neurons is not increased in anesthetized angiotensin II-salt hypertensive rats. *Am J Physiol Heart Circ Physiol*.

128. Pinault D (1996) A novel single-cell staining procedure performed in vivo under electrophysiological control: morpho-functional features of juxtacellularly labeled thalamic cells and other central neurons with biocytin or Neurobiotin. *J Neurosci Methods* 65:113-136.

129. Ray CA and Carter JR (2010) Effects of aerobic exercise training on sympathetic and renal responses to mental stress in humans. *Am J Physiol Heart Circ Physiol* 298:H229-H234.

130. Ross CA, Ruggiero DA, Joh TH, Park DH and Reis DJ (1984a) Rostral ventrolateral medulla: Selective projections to the thoracic autonomic cell column from the region containing C1 adrenaline neurons. *J Comp Neur* 228:168-185.

131. Ross CA, Ruggiero DA, Park DH, Joh TH, Sved AF, Fernandex-Pardal J, Saavedra JM and Reis DJ (1984b) Tonic vasomotor control by the rostal ventrolateral medulla: effect of electrical or chemical stimulation of the area containing C1 adrenaline neurons on arterial pressure, heart rate, and plasma catecholamines and vasopressin. *J Neurosci* 4:474-494.

132. Ruggiero DA, Cravo SL, Arango V and Reis DJ (1989) Central control of the circulation by the rostral ventrolateral reticular nucleus: anatomical substrates. *Prog Brain Res* 81:49-79.

133. Schreihofer AM and Guyenet PG (1997) Identification of C1 presympathetic neurons in rat rostral ventrolateral medulla by juxtacellular labeling *in vivo*. *J Comp Neurol* 387:524-536.

134. Schreihofer AM and Guyenet PG (2000a) Role of presympathetic C1 neurons in the sympatholytic and hypotensive effects of clonidine in rats. *Am J Physiol Regul Integr Comp Physiol* 279:R1753-R1762.

135. Schreihofer AM and Guyenet PG (2000b) Sympathetic reflexes after depletion of bulbospinal catecholaminergic neurons with anti-DbH-saporin. *Am J Physiol Regul Integr Comp Physiol* 279:R729-R742.

136. Schreihofer AM and Guyenet PG (2002) The baroreflex and beyond: control of sympathetic vasomotor tone by GABAergic neurons in the ventrolateral medulla. *Clin Exp Pharmacol Physiol* 29:514-521.

137. Schreihofer AM and Guyenet PG (2003) Baro-activated neurons with pulse-modulated activity in the rat caudal ventrolateral medulla express GAD67 mRNA. *J Neurophysiol: 8*91265-1277.

138. Schreihofer AM, Mandel DA, Mobley SC and Stepp DW (2007) Impairment of sympathetic baroreceptor reflexes in obese Zucker rats. *Am J Physiol Heart Circ Physiol* 293:H2543-H2549.

139. Schreihofer AM, Stornetta RL and Guyenet PG (1999) Evidence for glycinergic respiratory neurons: Botzinger neurons express mRNA for glycinergic transporter 2. *J Comp Neurol* 407:583-597.

140. Schreihofer AM, Stornetta RL and Guyenet PG (2000) Regulation of sympathetic tone and arterial pressure by rostral ventrolateral medulla after depletion of C1 cells in rat. *J Physiol* 529 Pt 1:221-236.

141. Schreihofer AM and Sved AF (2011) The ventrolateral medulla and sympathetic regulation of arterial pressure, in *Autonomic control of cardiovascular function* (Llewellyn-Smith IJ and Verberne AJM eds) pp 78-97, Oxford University Press, New York.

142. Senitko AN, Charkoudian N and Halliwill JR (2002) Influence of endurance exercise training status and gender on postexercise hypotension. *J Appl Physiol* 92:2368-2374.

143. Silva AQ and Schreihofer AM (2011) Altered sympathetic reflexes and vascular reactivity in rats after exposure to chronic intermittent hypoxia. *J Physiol* 589:1463-1476.

144. Southerland EM, Milhorn DM, Foreman RD, Linderoth B, DeJongste MJ, Armour JA, Subramanian V, Singh M, Singh K and Ardell JL (2007) Preemptive, but not reactive, spinal cord stimulation mitigates transient ischemia-induced myocardial infarction via cardiac adrenergic neurons. *Am J Physiol Heart Circ Physiol* 292:H311-H317.

145. Stocker SD, Cunningham JT and Toney GM (2004) Water deprivation increases Fos immunoreactivity in PVN autonomic nuerons with projections to the spinal cord and rostral ventrolateral medulla. *Am J Physiol Regul Integr Comp Physiol* 287:R1172-R1183.

146. Stocker SD, Simmons JR, Stornetta RL, Toney GM and Guyenet PG (2006) Water deprivation activates a glutamatergic projection from the hypothalamic paraventricular nucleus to the rostral ventrolateral medulla. *J Comp Neurol* 494:673-685.

147. Strack AM, Sawyer WB, Hughes JH, Platt KB and Loewy AD (1989) A general

pattern of CNS innervation of the sympathetic outflow demonstrated by transneuronal pseudorabies viral infections. *Brain Res* 491:156-162.

148. Subramanian M, Holt AG and Mueller PJ (2014) Physical activity correlates with glutamate receptor gene expression in spinally-projecting RVLM neurons: A laser capture microdissection study. *Brain Res* 1585:51-62.

149. Subramanian M and Mueller PJ (2016) Altered Differential Control of Sympathetic Outflow Following Sedentary Conditions: Role of Subregional Neuroplasticity in the RVLM. *Front Physiol* 7:290.

150. Takayama K, Suzuki T and Miura M (1994) The comparison of effects of various anesthetics on expression of Fos protein in the rat brain. *Neurosci Lett* 176:59-62.

151. Thom T, Haase N, Rosamond W, Howard VJ, Rumsfeld J, Manolio T, Zheng ZJ, Flegal K, O'Donnell C, Kittner S, Lloyd-Jones D, Goff DC, Hong Y, Adams R, Friday G, Furie K, Gorelick P, Kissela B, Marler J, Meigs J, Roger V, Sidney S, Sorlie P, Steinberger J, Wasserthiel-Smoller S, Wilson M, Wolf P and American Heart Association Statistics Committee and Stroke Statistics Subcommittee (2006) Heart disease and stroke statistics-2006 update: A report from the American Heart Association statistics committee and stroke statistics subcommittee. *Circulation* 113:e85-151.

152. Toney GM, Chen QH, Cato MJ and Stocker SD (2003) Central osmotic regulation of sympathetic nerve activity. *Acta Physiol Scand* 177:43-55.

153. Toney GM and Daws LC (2006) Juxtacellular Labeling and Chemical Phenotyping of Extracellular Recorded Neurons In Vivo, in *Ion Channels: Medthods and Protocols* (Stockand JD and Shapiro MS eds) pp 127-137,

Humana Press Inc., Totowa, NJ.

154. Ulyanova A, To XV, Asad AB, Han W and Chuang KH (2017) MEMRI detects neuronal activity and connectivity in hypothalamic neural circuit responding to leptin. *Neuroimage* 147:904-915.

155. Van de Moortele PF, Auerbach EJ, Olman C, Yacoub E, Ugurbil K and Moeller S (2009) T1 weighted brain images at 7 Tesla unbiased for Proton Density, T2* contrast and RF coil receive B1 sensitivity with simultaneous vessel visualization. *Neuroimage* 46:432-446.

156. Van der Linden A, Verhoye M, Van M, V, Tindemans I, Eens M, Absil P and Balthazart J (2002) In vivo manganese-enhanced magnetic resonance imaging reveals connections and functional properties of the songbird vocal control system. *Neuroscience* 112:467-474.

157. Verberne AJ and Sartor DM (2010) Rostroventrolateral medullary neurons modulate glucose homeostasis in the rat. *Am J Physiol Endocrinol Metab* 299:E802-E807.

158. Wang L, Lu H, Brown PL, Rea W, Vaupel B, Yang Y, Stein E and Shepard PD (2015) Manganese-Enhanced MRI Reflects Both Activity-Independent and Activity-Dependent Uptake within the Rat Habenulomesencephalic Pathway. *PLoS One* 10:e0127773.

159. Wendland MF (2004) Applications of manganese-enhanced magnetic resonance imaging (MEMRI) to imaging of the heart. *NMR Biomed* 17:581-594.

160. Weng JC, Chen JH, Yang PF and Tseng WY (2007) Functional mapping of rat barrel activation following whisker stimulation using activity-induced manganese-dependent contrast. *Neuroimage* 36:1179-1188.

161. Xu B, Zheng H and Patel KP (2012) Enhanced activation of RVLM-projecting PVN neurons in rats with chronic heart failure. *Am J Physiol Heart Circ Physiol* 302:H1700-H1711.

162. Zhang J and Mifflin SW (1997) Influences of excitatory amino acid receptor agonists on nucleus of the solitary tract neurons receiving aortic depressor nerve inputs. *J Pharmacol Exp Ther* 282:639-647.

163. Zheng W, Kim H and Zhao Q (2000) Comparative toxicokinetics of manganese chloride and methylcyclopentadienyl manganese tricarbonyl (MMT) in Sprague-Dawley rats. *Toxicol Sci* 54:295-301.

164. Zubcevic J, Jun JY, Kim S, Perez PD, Afzal A, Shan Z, Li W, Santisteban MM, Yuan W, Febo M, Mocco J, Feng Y, Scott E, Baekey DM and Raizada MK (2014) Altered inflammatory response is associated with an impaired autonomic input to the bone marrow in the spontaneously hypertensive rat. *Hypertension* 63:542-550.

165. Zucker IH, Patel KP, Schultz HD, Li Y-F, Wang W and Pliquett RU (2004) Exercise training and sympathetic regulation in experimental heart failure. *Exerc Sport Sci Rev* 32:107-111.

## ABSTRACT


**ACTIVITY DEPENDENT CHANGES IN FUNCTIONAL AND MORPHOLOGICAL CHARACTERISTICS AMONG PRESYMPATHETIC NEURONS OF THE ROSTRAL VENTROLATERAL MEDULLA**

by

**DANIEL JOSEPH HUERECA**

**August 2017**

**Advisor:** Patrick J. Mueller, Ph.D.

**Major:** Pharmacology

**Degree:** Doctor of Philosophy

A sedentary lifestyle is a major risk factor for the development of cardiovascular disease (CVD), the leading cause of death among Americans. Increasing evidence implicates increased sympathetic nerve activity (SNA) as the link between a sedentary lifestyle and CVD. The research presented in this dissertation examines the region of the brainstem known as the rostral ventrolateral medulla (RVLM) and how its regulation of SNA changes as a result of sedentary conditions. Our group has previously reported that sedentary conditions enhance splanchnic SNA in response to pharmacologically induced decreases in blood pressure or by direct activation of the RVLM via microinjection of the amino acid glutamate. More recently, our group has published the first evidence of overt structural differences in phenotypically identified RVLM neurons from sedentary versus physically active rats. Although collectively these studies suggest that a sedentary lifestyle results in increased activity and sensitivity of presympathetic RVLM neurons involved in blood pressure regulation, direct evidence of this proposed mechanism for the observed increased splanchnic SNA is lacking. The studies presented in this dissertation use *in vivo* characterization and juxtacellular

labeling of RVLM neurons to examine the potential mechanistic connection and physiological relevance of overt changes in their structure and function and how they relate to enhanced SNA in sedentary versus physically active rats. These cross sectional studies are complemented by longitudinally based studies of *in vivo* neuronal activity in the RVLM utilizing manganese-enhanced magnetic resonance imaging (MEMRI). The information gained from these studies will contribute to our understanding of how a sedentary lifestyle contributes to the development of CVD and may provide information on new therapeutic targets in the brain to prevent or slow the progression of CVD.

# AUTOBIOGRAPHICAL STATEMENT

## DANIEL JOSEPH HUERECA

**Education**

2017 Ph.D. (Pharmacology) Wayne State University School of Medicine, Detroit, MI
2001 B.S. (Biology) The University of Michigan, Ann Arbor, MI
1999 A.S. (Biology) Oakland Community College, Auburn Hills, MI

**Honors/Awards**

2016 Experimental Biology Meeting, APS Data NCARnation Speaker, APS
2016 Experimental Biology Meeting, Minority Travel Fellowship Award, APS
2015-2017 Predoctoral Fellowship, American Heart Association 07/01/15-06/30/17 15PRE25700308 ($130,000)
2015 Outstanding Oral Presentation, 2015 Michigan Physiological Society Meeting
2013-2014, 2014-2015 Rumble Fellowship, Wayne State University
2014 Outstanding Poster, 2014 Michigan Physiological Society Meeting
2014 Experimental Biology Meeting, Minority Travel Fellowship Award, APS
2012 NIDA Travel Award, 25th Anniversary Serotonin Club Meeting
2011-2013 IMSD Graduate Fellowship, Wayne State University
2010-2011 Graduate Research Fellowship, Wayne State University School of Medicine

**Teaching/Service**

2016 Meeting Mentor - Experimental Biology 2016 Meeting
2015, 2016 PhUn Speaker – Physiology Understanding Week, American Physiological Society
2013 Host, Student President - 40th Annual Pharmacology Colloquium
2012, 2013 Lecturer, Wayne State University Initiative for Maximizing Student Diversity
2011 Guest Lecturer, Wayne State University School of Medicine, Drugs and the Addictive Process
2001, 2002, Undergraduate Instructor, University of Michigan Math and Science Scholars

**Publications**

1. **Huereca D***, Bakoulas K*, Ghoddoussi F, Berkowitz B, Holt A, Mueller P. Development of Manganese-Enhanced Magnetic Resonance Imaging of the Rostral Ventrolateral Medulla of Conscious Rats: Importance of Normalization and Comparison to Other Regions of Interest. NMR Biomed. 2017 (***In Revision***).
2. Andrade R, **Huereca D**, Lyons J, Andrade E, McGregor K. 5-HT1A Receptor-Mediated Autoinhibition and the Control of Serotonergic Cell Firing. ACS Chem Neurosci. 2015 Jul 15;6(7):1110-5.

**Abstracts**

1. **Huereca, D.J**., Holt, A.G., Berkowitz, B.A., Mueller, P.J., Developing manganese-enhanced MRI as a non-invasive measure of *in vivo* neuronal activity in the rostral ventrolateral medulla (RVLM) of sedentary and physically active rats. Experimental Biology Meeting, San Diego, CA, USA FASEB J APRIL 2016 30:756.3
2. **Huereca, D.J.**, Barman, S.M., Mueller, P.J., Spectral analysis of barosensitive neurons in the rat rostral ventrolateral medulla. FASEB J April 2015 29:649.12
3. **Huereca, D.J.**, Wong, C.K., Ingles, J.A., Ghoddoussi, F., Berkowitz, B.A., Holt, A.G., Mueller, P.J., Assessment of neuronal activity in the rostral ventrolateral medulla (RVLM) of conscious rats. FASEB J April 2015 29:652.8
4. **Huereca, D.J.**, Mueller, P.J., Single unit recordings from putative presympathetic neurons in the rostral ventrolateral medulla (RVLM) of sedentary and physically active rats. FASEB J 28:686.35, 2014.
5. Ingles, J.A., **Huereca, D.J**., Holt, A.G., Mueller, P.J., Functional studies of rostral ventrolateral medulla neurons using manganese-enhanced magnetic resonance imaging in sedentary versus physically active rats. FASEB J April 2014 28:686.36
6. **Huereca, D.J**., Andrade, R., Channelrhodopsin reveals robust 5-HT1A receptor mediated autoinhibition in the dorsal raphe, 42nd Annual Meeting of the Society for Neuroscience, New Orleans, LA, USA. 10/2012
7. **Huereca, D.J**., Andrade, R., Autoinhibition in the dorsal raphe is mediated by local release of serotonin, Serotonin Club Meeting, Faculté de médecine de Montpellier, Montpellier, France. 07/2012